

Stimuli-responsive Compounds as Emerging Anticancer and Cell Imaging Agents

Deepti U. Kirtani and Anupa A. Kumbhar*

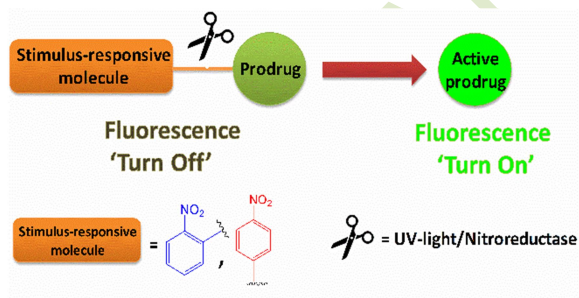
Department of Chemistry, Savitribai Phule Pune University, Ganeshkhind Road, Pune-411007, India.
Email: anupa.kumbhar@unipune.ac.in

Received: March 24, 2023 | Accepted: June 06, 2023 | Published online: July 31, 2023

Abstract

Discovery of cisplatin furthered the development of many platinum and non-platinum drugs for anticancer and cell imaging applications. However, non-selective nature of these drugs exert toxicity to both, cancer and normal cells. This review focuses on use of external stimuli viz. UV-light and enzyme nitroreductase to release the drugs specifically in cancer cells to exert anticancer activity as well as release a fluorophore for imaging hypoxic cells.

Keywords: Anticancer agents, imaging agents, nitroreductase, photoactive, stimulus-responsive



1. Introduction

Cancer is one of the second most fatal diseases responsible for 21 to 25% annual deaths globally.^{1,2} It is mainly characterized by uncontrolled growth of abnormal cells with an ability to spread all over the body leading to metastasis.² As shown in the Figure 1, during the normal cell proliferation if the cell is damaged or defected then the cell either repairs itself or dies by the mechanism called apoptosis.³ In-contrast, if the abnormal cell continues to grow it develops into a tumor.⁴ Tumors cells have low levels of oxygen (1% to 2% of O₂) than normal cells.⁵⁻¹⁰ These cells are aggressive and adapt to cellular environmental stress, escape apoptosis and survive.^{11,12} This leads to genetic instability, malignant progression in cells and resistance to therapy.^{7,13-15}

Metals and metal complexes have been used in various medical applications from thousands of years.^{16,17} In metal-based drugs, central metal ion is the key feature for the mechanism of action.¹⁸ Inorganic metal complexes due to their variety of coordination sphere, oxidation states, ligand design, and redox states alter the responsiveness of the compounds towards biological activity.¹⁸ In the early 1900's potassium dicyanoaurate and antimony were used to treat tuberculosis and leishmaniasis respectively.¹⁷ In addition, gold salts and arsenic compounds were also used for treating bacterial infections.¹⁷ Cis-diamminedichloroplatinum(II) (cisplatin, **1**) was first synthesized by Michele Peyrone in 19th century and by 20th century the accidental discovery of cisplatin for anticancer property by Barnette Rosenberg led a corner stone for treatment of cancer.^{17,19} Cisplatin was found to be effective in the treatment of variety of cancers such as testicular, ovarian, colorectal, bladder, non-small cell lung and head and neck cancers.^{20,21} Being an effective anticancer drug it also came with lot of drawbacks such as dose-limiting

toxicity, intrinsic tumor resistance, nausea, vomiting, toxicity towards normal cells including neurotoxicity, ototoxicity and nephrotoxicity.^{20,22,23} These limitations prompted the development of new platinum drugs with chemotherapeutic properties in treatment of cancer.²¹

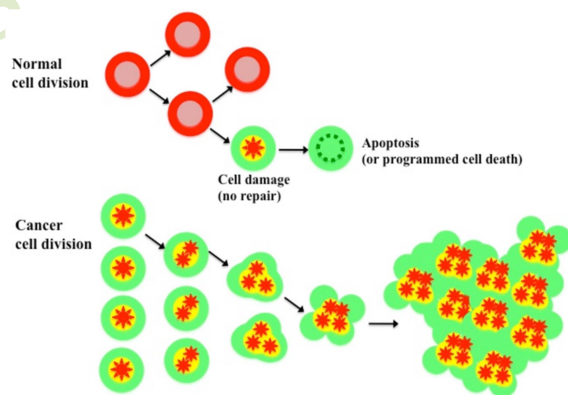


Figure 1. Schematic representation of normal versus cancer cell division. Adapted from reference².

To improve the efficacy, second (changing the leaving group) and third (changing the amines) generation cisplatin analogues were synthesized by modifying the coordination environment around the platinum centre.^{24,25} Carboplatin²⁶ and nedaplatin^{19,27} were the second generation platinum based drugs. Carboplatin was developed to improve dose-limiting toxicity of cisplatin. Major drawback of carboplatin myelosuppression and limited efficacy for most of the cancers was noted.²⁸ Nedaplatin exhibited improved pharmacokinetic properties with reduced nephrotoxicity. It has been approved in Japan for the treatment of esophageal, neck, head, small cell and non-small cell lung cancers.²⁹ However, side-effects like dose-limiting toxicity,

myelosuppression and abnormal functioning of renal system was observed.²⁰

Oxaliplatin, lobaplatin and heptaplatin are the third generation of cisplatin analogues.^{19,29} Oxaliplatin is approved to treat the colorectal cancer worldwide.³⁰ Lobaplatin and heptaplatin have received regional acceptance in China and Korea.³¹ Lobaplatin does not induce renal-, neuro- or ototoxicity, however, it triggered anemia and leukopenia.^{32–36} Lobaplatin is currently used in the treatment of chronic myelogenous leukaemia, metastatic breast cancer and small cell lung cancer.³⁷ Heptaplatin is used in the treatment of gastric cancers, and shows severe nausea, hepatotoxicity and nephrotoxicity.^{38–40} The toxic side effects such as neutropenia, emesis and proteinuria were found to be lowered when heptaplatin was used for the treatment.⁴¹ There are few platinum-based drugs which recently entered clinical trials.

In picoplatin, pyridine ring was introduced to create steric hindrance to prevent the attack of nucleophiles, mainly thiols.^{42,43} Although picoplatin was useful on resistant cell lines without nephrotoxicity, it was withdrawn from phase II clinical trials as it was found to be ineffective in curbing the disease progression especially in non-small cell lung cancer and small cell lung cancers.^{44–46} Picoplatin is currently undergoing phase I and phase II clinical trials on colorectal cancer in combination with 5-fluorouracil and leucovorin, and prostate cancer in combination with docetaxel.⁴⁷ Satraplatin was found effective against cisplatin-resistant cancers including human lung, ovary, cervix and prostate cancer.^{48–50} Clinical trials revealed that it was effective against the patients with refractory cancer, prostate cancer and squamous cell carcinoma of the head and neck.^{50,51} However, satraplatin was rejected by FDA as it showed less convincing results in terms of overall survival of patients.⁵¹ LA12 is the analogue of satraplatin.^{52,53} It showed higher uptake in cisplatin-resistant cell lines and recently completed phase I trial.^{48,54} ProLindac^{55–59} is a combination of active oxaliplatin conjugated with hydrophilic biocompatible polymer, hydroxypropylmethacrylamide. This drug targets solid tumors with increased permeability and retention effect. *In-vitro* studies of ProLindac revealed 20 times higher platinum-adducts at pH 3.0 than pH 7.4. This explains the enhanced activity of ProLindac on hypoxic tumors as they have low extracellular pH. In phase I studies, ProLindac showed antiproliferative activity on metastatic melanoma and in advanced ovarian cancer patients.⁶⁰ This drug is in phase II clinical trial for treatment of ovarian cancer.⁵⁶ Figure 2 summarizes the strategies used in the development of second and third generation platinum-based drugs.⁶¹

Although these platinum complexes were showing anticancer properties on various cancer cell lines and tumors, they suffered from many limitations with severe side-effects, poor selectivity and development of resistance. Cisplatin and other platinum-based drugs covalently bind to DNA (Figure 3), mostly to guanine and adenosine nucleobases. This leads to inhibition of DNA synthesis and ultimately cell death.^{62,63} The shortcomings of platinum drugs

eventually restricted their use in the treatment of cancer. These unresolved problems of platinum anticancer drugs stimulated efforts to develop non-platinum based antineoplastic agents.

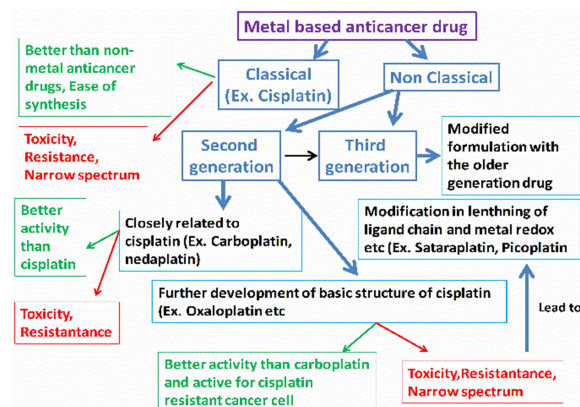


Figure 2. Flow chart of development of platinum based anticancer drugs (Green arrow indicates advantage and red arrow shows disadvantage). Adapted from reference.⁶¹

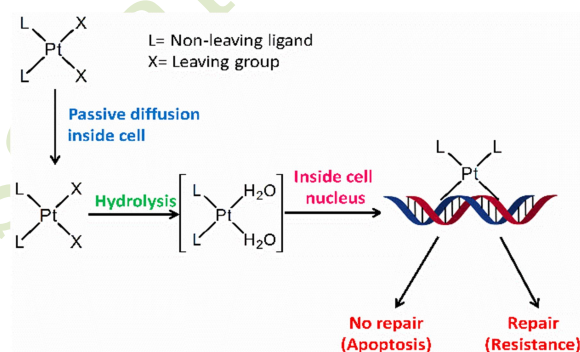


Figure 3. Mechanism of anticancer activity of platinum complexes. Adapted from reference.^{62,63}

1.1 Non-platinum based anti-proliferative drugs

Metal-based anticancer compounds other than platinum were also been demonstrated as promising anticancer drugs. In addition, interest in developing more non-platinum based chemotherapeutics has increased as some of them have shown ability in treating variety of cancer strains with fewer side effects. Non-platinum transition metal complexes have advantages like variable oxidation states, tuning of redox potentials, electronic and physicochemical properties based on ligand scaffold, charge on the complex and geometry. This makes them active candidates in the field of medicinal chemistry for the treatment of cancer.^{64,65}

Transition-metals such as copper, iron, zinc and manganese are present at the active sites of proteins and enzymes and play an important role in biological processes like electron transfer and catalysis.⁶⁶ Reactive oxygen species (ROS) are generally unstable, highly reactive and partially reduced oxygen species which are byproducts of metabolic processes.^{67,68} It has been noted that ROS can be either tumor-supporting or tumor-suppressing agents.⁶⁹ Most of the

chemotherapeutics that generate ROS can trigger the cell death and are considered tumor suppressors.⁷⁰ The redox properties of both ligand and metal ions in transition-metal complexes offer routes for redox activation in hypoxic environment of tumor cells (Figure 4).⁷¹ Among the transition metal ions, copper and iron are well known for their redox active nature.⁷¹⁻⁷³ Both produce ROS via Fenton-like reaction to generate oxidative stress and promote cell death.^{74,75} So far, not a single non-platinum drug is approved for cancer therapy providing a great opportunity for continuous development of new drug molecules.⁷⁶ Some non-platinum complexes of ruthenium(II), titanium(IV), gallium(III), cobalt(II/III), iron(II/III), copper(I/II) etc. have displayed promising results in preclinical and clinical trials (Figure 5) and only those are discussed below.⁷⁶

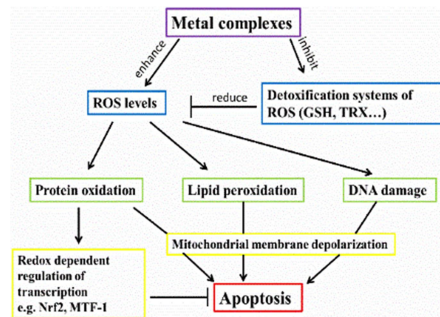
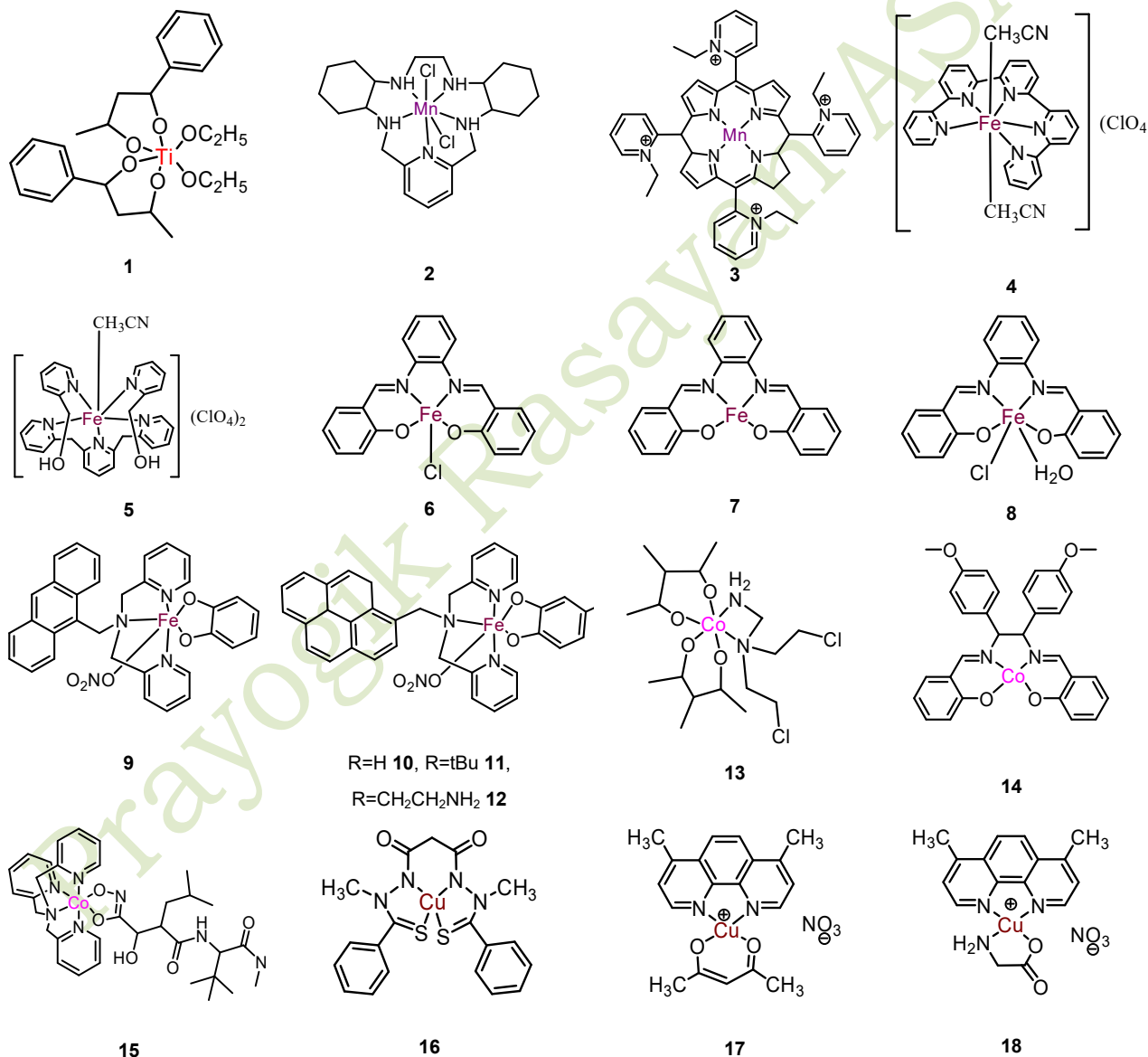


Figure 4. Overview of mechanism of anticancer activity of non-platinum complexes via generation of ROS. Adapted from reference⁶⁸.



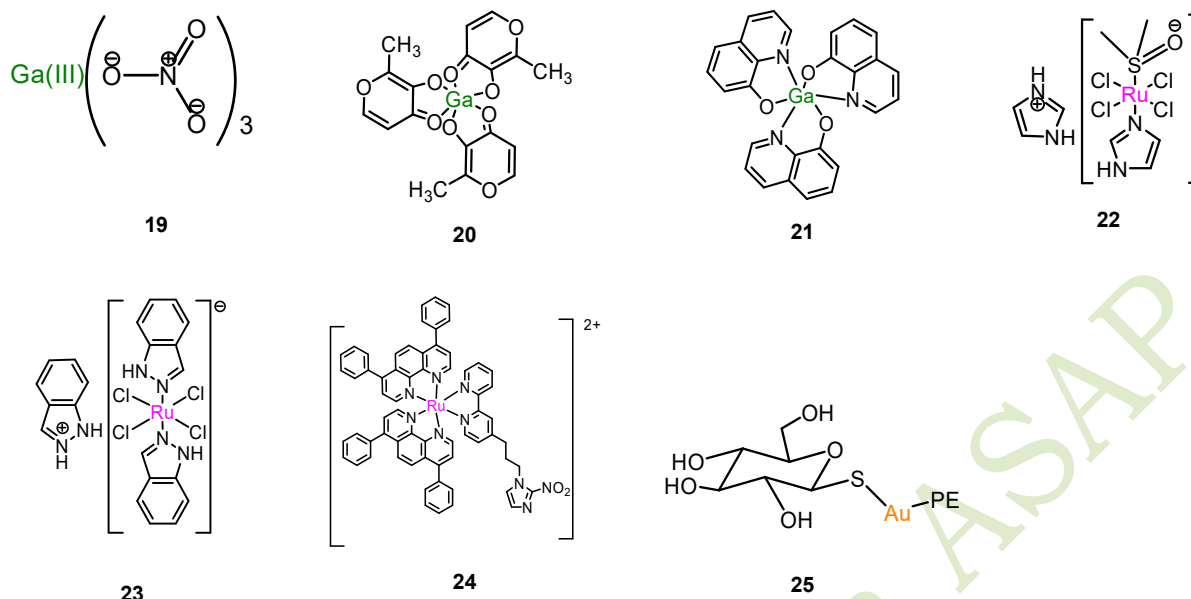


Figure 5. Chemical structures of antiproliferative non-platinum transition-metal complexes that are in clinical trials.

Titanium complex, budotitane $[(\text{bzac})_2\text{Ti}(\text{OEt})_2]$, **1** where bzac= 1-phenylbutane-1,3-diketonate was the first non-platinum drug which entered clinical trials.⁷⁷ Titanium complexes exhibited cytotoxicity on wide variety of cancer cells, by interacting with DNA and triggering apoptosis.⁷⁸⁻⁸³ It failed in preclinical trials due to lack of solubility in water and hydrolytic instability under physiological conditions.^{78,79}

Manganese is used as a cofactor in several biological processes including proteins and enzymes.^{66,84} Avasopasem ((2,6,8,11-tetraaza-4(2,6)-pyridina-1,7(1,2)-dicyclohexana cycloundecaphane, **2**) and MnTE-2-PyP^{5+} (2,2',2'',2'''-(4Z,6E,15E,19E)-1H,2H,3H,9H,10H,20H-porphyrin-5,10,15,20-tetrayl) tetrakis(1-ethylpyridin-1-ium) manganese(II), **3**) are Mn-based complexes that reached clinical trials for treatment of head and neck cancer, which are SOD mimics and act by scavenging the free radical formation in cells.⁸⁵⁻⁸⁷

Iron is essential in many biological processes including DNA synthesis, cell proliferation and growth. It is also present in hemoglobin, leghemoglobin and myoglobin.^{24,88} Iron mainly exists in two main ferrous (II) and ferric (III).⁸⁹ The change in oxidation states from Fe(II) to Fe(III) can produce ROS which are potentially toxic to cancer cells.^{24,90} The pentadentate *N*-donor complexes of iron(II), $[\text{Fe}(\text{H-qpy})(\text{CH}_3\text{CN})_2](\text{ClO}_4)_2$ (2,2':6',2'':6'',2''':6''',2''''-quinque pyridine di(acetonitrile) iron(II) chlorate, **4**), $[\text{Fe}(\text{Py5-OH})(\text{CH}_3\text{CN})_2]^{2+}$ (2,6-bis(pyridin-2-ylmethyl) pyridine bis(pyridin-2-ylmethanol) monoacetonitrile iron(II) chlorate, **5**) showed high toxicity (IC_{50} = 0.6-3.4 μM) by inducing apoptosis associated with DNA damage and cell cycle arrest.^{91,92} $[\text{Fe}(\text{III})\text{-(salophene)Cl}]$ (2, 2'-((1E, 1'E)-(1, 2-phenylenebis(azaneylylidene))bis(methaneylylidene)) diphenol iron(II) chloride,**6**) and $[\text{Fe}(\text{III})\text{ (salophene)}]$ (bis(azaneylylidene)) bis(methaneylylidene)) diphenol

Fe(III), **7**) inhibit the growth of tumors (MCF-7, MDA-MB-231, HT-29) and induce apoptosis.^{93,94} The complex $[\text{Fe}(\text{III})(\text{salophene})\text{Cl}\cdot\text{H}_2\text{O}]$ (bis(azaneylylidene)) bis(methaneylylidene)diphenol)iron(II) chloride monohydrate, **8**) was found to be highly toxic to ovarian cancer cell lines (IC_{50} = 300 nM) and neuroblastoma.^{94,95} It induces apoptosis by blocking the cells in S-phase of cell cycle. Further, the catecholates of Fe(III) complexes such as (anthracen-9-yl)-*N*, *N*-bis[(pyridin-2-yl)methyl] methanamine **9**, (pyrenyl-1-yl)-*N*, *N*-bis[(pyridin-2-yl)methyl] methanamine **10**, 4-tert-butyl catecholates **11**, 4-(2-aminoethyl) benzene-1, 2-diolate,**12** containing polyaromatic groups were found to be active in photodynamic therapy.⁹⁶⁻⁹⁸ These complexes displayed enhanced cytotoxicity to HeLa cell line when irradiated in visible (400-700 nm) or red (600-750 nm) light region.

Cobalt⁹⁹ is essential in biological processes and mainly found in Vitamin B12 (cobalamin). Cobalamin is involved in the formation of red blood cells, DNA synthesis and regulation, and maintenance of normal brain function. Being essential metal it is expected to cause less harm to human cells than non-essential metal like platinum.¹⁰⁰ Bis(3-methyl-2, 4-pentadionato)-*N*, *N'*-bis(2-chloroethyl) ethylenediamine cobalt(III), **13**) coordinated to nitrogen mustard ligand has shown to be hypoxia selective agent.^{101,102} Schiff-base *N*, *N'* ethylene bis(salicyclimine) cobalt(III) **14**) also exhibited anticancer activity similar to that of cisplatin.¹⁰³ Another complex $[\text{Co}(\text{mmst})\text{tpa}][\text{ClO}_4\cdot 4\text{H}_2\text{O}]$ (mmstH₂= marimastat); (tris(pyridin-2-ylmethyl)amine) ((*Z*)-3-((3, 3-dimethyl-1-(methylamino)-1-oxobutan-2-yl)carbamoyl)-*N*, 2-dihydroxy-5-methyl hexanimidic acid) Co(III), **15**) exerts its anticancer activity by acting on metalloproteinase. Upon reduction this complex inhibited the growth of mammary carcinoma.¹⁰⁴

Copper is an essential element required for biological processes in living organisms.²⁴ It is more toxic to cancer cells as compared to normal cells.¹⁰⁵ Copper complexes exhibit anticancer activity by generating ROS leading to ROS-mediated autophagy and apoptosis.¹⁰⁶ Cu(II) elesclomol (*N*¹, *N*³-dimethyl-*N*¹, *N*³-di(phenylcarbonothioyl) malonohydrazide) Cu(II), **16**)^{107–109} was the first complex to enter the clinical trials to treat acute myeloid leukemia. This drug was in phase II clinical trials for ovarian, fallopian and peritoneal cancers in phase II clinical trials. It acts by inducing DNA strand scission mediated by ROS in malignant cells. Casiopeina IIIa ((4,7-dimethyl-1, 10-phenanthroline) ((*Z*)-4-hydroxypent-3-en-2-one) Cu(II) nitrate, **17**)¹¹⁰ is also a copper(II) complex entered in phase I clinical trial as a putative agent for the treatment of acute myeloid leukemia. The mechanism of action involves DNA cleavage caused by ROS. Casiopeina II-Gly ((*Z*)-4-hydroxypent-3-en-2-one) glycine copper(II) nitrate, **18**)¹¹¹ also entered the clinical trials and was shown to block the migration and proliferation of HeLa cells.

Gallium is less toxic and has an ability to inhibit DNA synthesis. The anticancer property of gallium salts were discovered in 1971.¹¹² Gallium nitrate, **19** was the first gallium compound to enter phase II clinical trials.^{113,114} It showed antiproliferative activity against chronic lymphocytic leukemia, breast, bladder, renal, melanoma, prostate, lung, ovarian, and cervical cancers. However, patients treated with this drug showed partial response towards treatment. The next two generations of gallium compounds are gallium maltolate,**20** and tris(8-quinolato) gallium (III), KP46,**21**.^{17,115,116} Preclinical investigation of gallium maltolate showed activity against hepatoma, lymphoma and bladder cancers. **21** is currently in clinical trials as an oral gallium compound that exhibited inhibition of solid tumors like renal, ovarian, stomach and parotid gland.

Ruthenium (III) complexes were found to be less toxic, more selective towards cancer cells and possess antimetastatic activity.²⁴ Among various ruthenium(II) complexes, imidazolium-trans tetrachloro (dimethylsulfoxide) imidazole ruthenium (III), (NAMI-A, **22**), trans-[tetrachloro bis(1H-indazole) ruthenate(III)] (KP1019, **23**) and [Ru(4, 4'-dimethyl-2, 2'-bipyridine)₂ (2-(2', 2'': 5'',2''-terthiophene)-imidazo[4, 5-f])Cl₂ (TLD1433), **24**) entered the clinical trials. **22** displayed anti-angiogenic and anti-metastatic properties whereas **23** showed DNA damage and apoptosis induced by oxidative stress.

Several **gold(I)** complexes showed antiproliferative activity, targeting mitochondrial DNA.^{117,118} Among them auranofin,**25** is in clinical trials for the treatment of leukaemia.¹¹⁹

Researchers have designed countless metal-based anticancer agents with diverse coordination geometries and ligand systems acting on different cellular targets and mechanism of action. To summarize the mechanism of action of non-platinum complexes, almost all those discussed above exert their anticancer activity, with DNA as the main target, by invoking oxidative stress. Apart from that,

lipid peroxidation, disruption of mitochondrial membrane potential, inhibition of a particular growth phase in the cell-cycle, etc. are other modes responsible for cell death.

Many strategies are adapted to minimize toxicity and increase the efficacy of metal-based therapeutics. To achieve target specificity, the complexes are (i) tagged with tumor specific peptides or monoclonal antibodies, (ii) modified to tune the redox potential so as to reach the hypoxic tumors, or (iii) subjected to different stimuli such as pH, radiation, enzymatic dissociation etc. for controlled release of metal ion or drug to the specific tissue. This review focuses on compounds that can act as antiproliferative and imaging agents by responding to external stimuli to exert their activity.

Tumor targeting strategies that respond to external stimulus can enhance their selectivity to the target.¹²⁰ Stimulus responsive drug delivery system can prevent premature release of active component and ensure stability in biological systems until the respective stimulus is applied at the cellular sites.¹²¹ Further, by tagging the stimulus responsive molecule with a fluorescent probe one can monitor the distribution and binding of drugs to biomolecules in living systems. Hence, fluorescence microscopy become an important tool in real-time imaging of live cells with high sensitivity and selectivity.^{122,123} Here we have focused on the *o*-nitrophenyl and *p*-nitrophenyl moieties which act as activators in presence of UV-light and nitroreductase enzyme to behave as anticancer and imaging agents respectively. The readers can also refer to the reviews published earlier on the photocaged and nitroreductase sensing molecules.^{124–126}

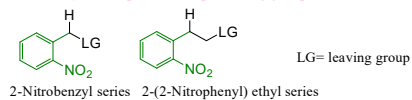
2. *Ortho*-nitrophenyl groups as photolabile protecting groups

Light is a highly selective and ideal external trigger and harmless to biological systems if applied correctly.¹²⁷ Therefore, a large number of photoactive compounds were discovered and used in various applications in the past few decades.¹²⁸ They have received considerable attention for the controlled delivery of active components with the help of light.^{129,130} Photoactivated drugs^{131,132} are mostly employed in photodynamic therapy which uses photosensitive molecules and light of a specific wavelength as a trigger to release the drug molecules at a specific site.¹³³ A collection of such photolabile protecting groups is given in Figure 6. An ideal photoactive compound must possess greater stability under physiological conditions, efficient release and good aqueous solubility of photoproduct(s) and faster photocleavage kinetics.^{127,134}

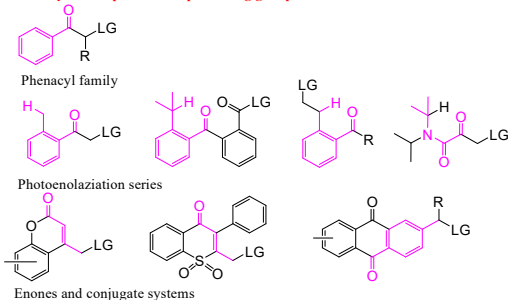
Among the various photoactive groups, *o*-nitrophenyl derivatives are most common because of their versatility, compatibility with various functional groups (phosphates, carboxylates, hydroxyl groups, amines and amides) and good light sensitivity.^{135,136} *o*-Nitrophenyl compounds absorbs between 300-360 nm for efficient photolysis.¹³⁷ The UVA range (315-400 nm) indirectly damages the DNA and other cellular components by formation of ROS in cellular

components.¹³⁸ Therefore it is essential for efficient photolysis to decrease the light toxicity. Hence quantum efficiency and its extinction coefficient at the irradiation wavelength become the two defining properties of photolabile groups. Hence by increasing the photolysis efficiency, one can lower the exposure time.

Nitrobenzyl based photolabile protecting groups



Carbonyl based photolabile protecting groups



Benzyl based photolabile protecting groups

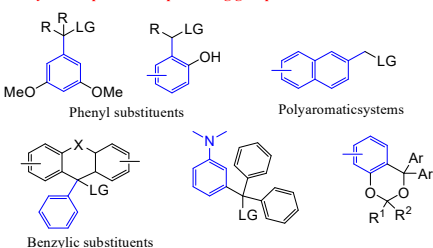
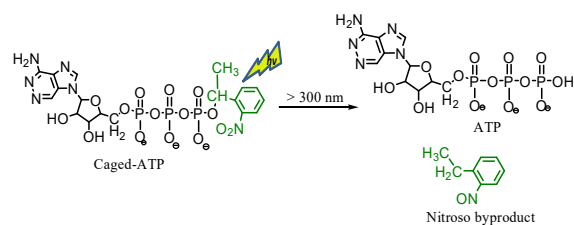
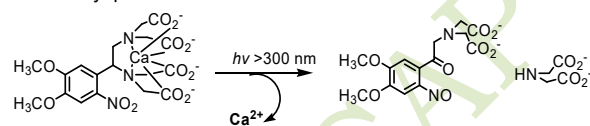


Figure 6. Chemical structures of molecules with photolabile protecting groups.

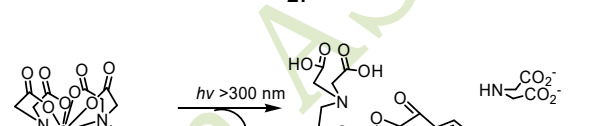


26

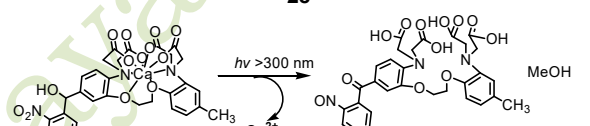
Figure 7. Schematic presentation of photolysis mechanism of nitrobenzyl protected-ATP molecule.



27

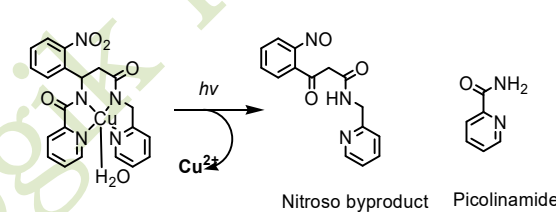


28



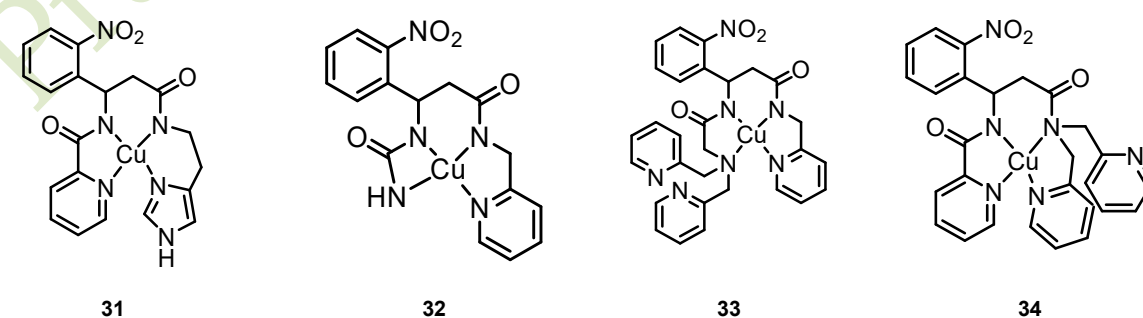
29

Figure 8. Photochemistry of caged calcium complexes depicting release of Ca(II) ion on light activation.



30

Figure 9. Light activation uncaging of Cu(II) complex with low affinity for Cu(II).



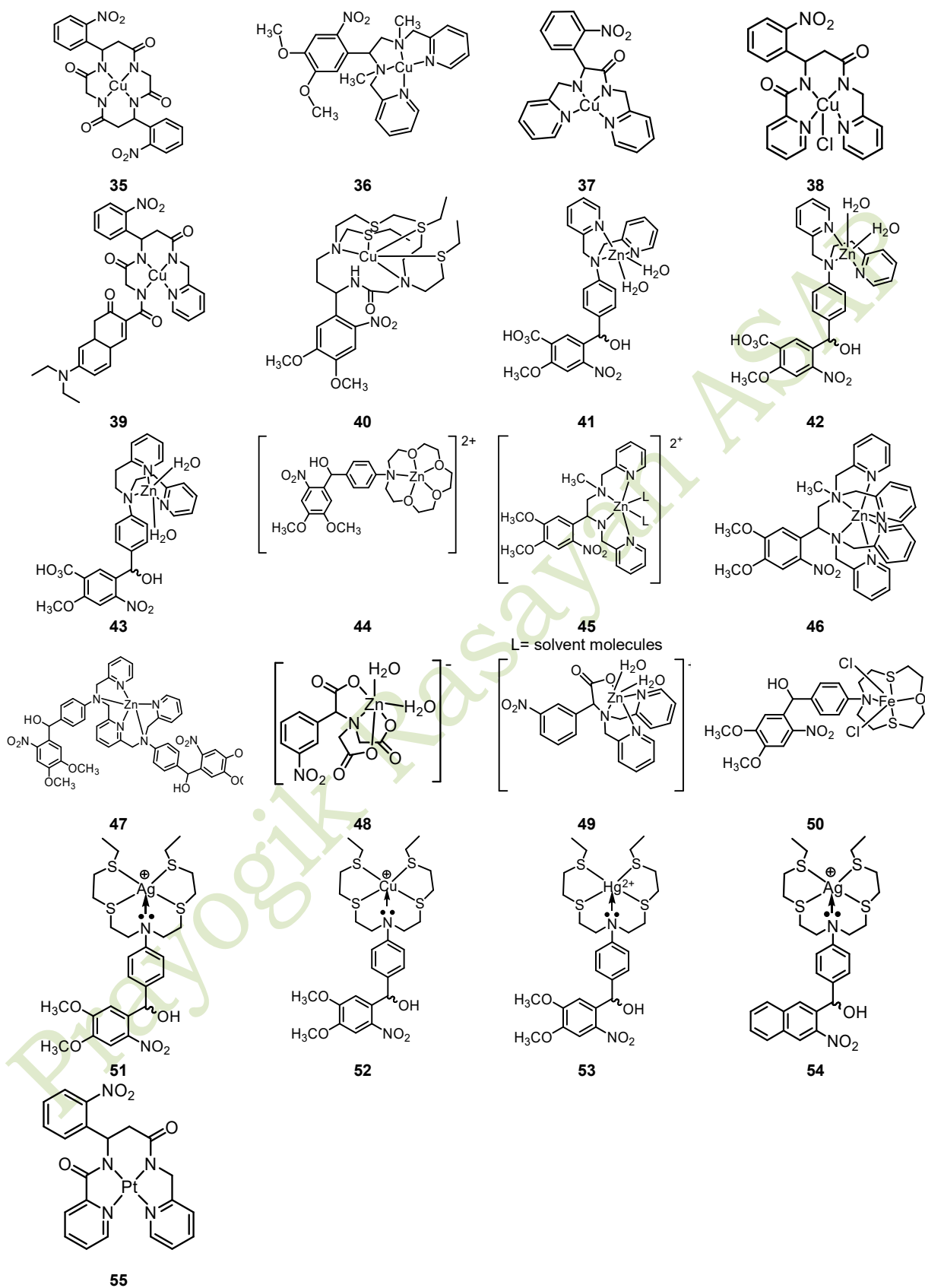


Figure 10. Chemical structures of transition-metal caged complexes.

Table 1 Photophysical properties of photoactive metal complexes.

Sr.No	Compound, chemical name	λ_{ex}	λ_{em}	Solvent	K_d (M)	$\phi_{\text{photolysis}}$
1.	30 , Pyridine-2-carboxylic acid {1-(2-nitro-phenyl)-2-[(pyridine-2-ylmethyl)-carbamoyl]-ethyl}-amide) aqua copper(II) complex	580nm	NR	20mM NaH ₂ PO ₄ buffer pH 7.4	1.6×10^{-11}	73%
2.	31 , 2-Methyleneamino-but-2-enoic acid [2-[2-(1H-imidazol-4-yl)-ethylcarbamoyl]-1-(2-nitro-phenyl)-ethyl]-amidocopper(II) complex	NR	NR	NR	NR	NR
3.	32 , 3-(2-Amino-acetyl-amino)-3-(2-nitro-phenyl)-N-pyridin-2-ylmethyl-propionamide copper(II) complex	NR	NR	Phosphate buffer pH 7.4	2×10^{-10}	NA
4.	33 , 3-[2-(Bis-pyridin-2-ylmethyl-amino)-acetyl-amino]-3-(2-nitrophenyl)-N-pyridin-2-ylmethyl-propionamide copper(II) complex	NR	NR	NR	NR	NR
5.	34 , Pyridine-2-carboxylic acid [2-(bis-pyridin-2-ylmethylcarbamoyl)-1-(2-nitro-phenyl)-ethyl]-amide copper(II) complex	NR	NR	NR	NR	NR
6.	35 , 7,14-Bis-(2-nitro-phenyl)-1,4,8,11-tetraaza-cyclotetradecane-2,5,9,12-tetraone copper(II) complex	NR	NR	NR	NR	NR
7.	36 , (1-(4,5-dimethoxy-2-nitro-phenyl)-N,N'-dimethyl-N,N'-bispyridin-2-ylmethyl-ethane-1,2-diamine) copper(II) complex	NR	NR	Phosphate buffer pH 7.4	5×10^{-17}	0.55%
8.	37 , 2-(2-Nitro-phenyl)-N-pyridin-2-ylmethyl-2-[(pyridin-2-ylmethyl)-amino]-acetamide copper(II) complex	NR	NR	NR	NR	NR
9.	38 , Pyridine-2-carboxylic acid {1-(2-nitrophenyl)-3-[(pyridine-2-ylmethyl)-amino]-propyl}-amide)chloride copper(II) complex	584nm	NR	PBS buffer pH 7.4	2×10^{-16}	66%
10.	39 , 7-Diethylamino-2-oxo-2H-chromene-3-carboxylic acid ({1-(2-nitro-phenyl)-2-[(pyridin-2-ylmethyl)-carbamoyl]-ethylcarbamoyl}-methyl)-amide copper(II) complex	432nm	479nm	10mM HEPES buffer pH7.4 10% DMSO	7.3×10^{-6}	1.6%
11.	40 , 2-(Bis(2-(ethylthio)ethyl)amino)-N-(3-(bis(2(ethylthio)ethyl)amino)-1-(4,5-dimethoxy-2-nitrophenyl)propyl)acetamide copper(I) complex	420nm	560nm	20mM HEPES buffer, 100mM KCl, 30% EtOH, pH 7.0	5.4×10^{-11}	1.1%
12.	41 , 4-(Bis-pyridin-2-ylmethylamino)phenyl] (4,5-dimethoxy-2-nitrophenyl) zinc(II) complex	350nm	NR	MeCN EtOH	9.7×10^{-6} 1.3×10^{-5}	0.3% 2.2%

				50mM HEPES buffer, 100mM KCl, pH 7.0, 20% EtOH	6.1×10^{-5}	0.5%
13.	42 , (4,5-Dimethoxy-2-nitrophenyl)(4-([2-(pyridine-2-yl)ethyl](pyridine-2-ylmethyl)amino)phenyl) zinc(II) complex	350nm	NR	MeCN	8.6×10^{-6}	0.4%
				EtOH	2.5×10^{-4}	1.8%
14.	43 , (4-(Bis[2-(pyridine-2-yl)ethyl]amino) phenyl)(4,5-dimethoxy-2-nitrophenyl) zinc(II) complex	350nm	NR	EtOH	3.1×10^{-3}	NR
15.	44 , [4-(1-aza-15-crown-5)phenyl]-(4,5-dimethoxy-2-nitrophenyl)-methanol zinc(II) complex	347nm	NR	MeCN	1.61×10^{-4}	1.6%
16.	45 , 1-(4,5-dimethoxy-2-nitrophenyl)-N, N'-dimethyl-N, N'-bispyridin-2-ylmethyl-ethane-1, 2-diamine) zinc(II) complex	360nm	540nm	40mM HEPES buffer, 100mM KCl, pH 7.0	2.3×10^{-13}	0.55%
17.	46 , 1-(4, 5-dimethoxy-2-nitrophenyl)-N, N, N', N'-tetrakis-pyridin-2-ylmethyl-ethane-1, 2-diamine)) zinc(II) complex	350nm	440nm	40mM HEPES buffer, 100mM KCl, pH 7.0	9×10^{-16}	2.3%
18.	47 , [4-(bis-pyridin-2-ylmethyl-amino)-phenyl]-(4,5-dimethoxy-2-nitro-phenyl) zinc(II) complex	270nm	NR	MeCN	1.2×10^{-5}	NR
19.	48 , 2,2'-(carboxy(3-nitrophenyl) methyl) azanediyl) diacetic acid) zinc(II) complex	274nm	NR	40mM HEPES buffer, 100mM KCl, pH 7.5	1×10^{-13}	27%
20.	49 , 2,2'-(carboxy(3-nitrophenyl)methyl) azanediyl) diacetic acid) zinc(II) complex	347nm	512nm	40mM HEPES buffer, 100mM KCl, 10% MeCN pH 7.5	8×10^{-13}	27%
21.	50 , 4-(1-oxa-4, 10-dithia-7-azacyclodo decan-7-yl)phenyl)(4, 5-dimethoxy-2-nitrophenyl)methanol) iron(III) complex	350nm	NR	MeCN	NR	4%
22.	51 , (4-(Bis(2-(2-(Ethylthio)ethyl)thio) ethyl)amino)phenyl)(4,5-dimethoxy-2-nitrophenyl)methanol silver(I) complex	350nm	NR	MeCN	0.0114	0.92%
				MeOH	0.0119	1.5%
				20mM HEPES buffer/ dioxane (1:1), pH 7.0	0.009	1.4%
23.	52 , (4-(Bis(2-(2-(Ethylthio)ethyl)thio) ethyl)amino)phenyl)(4,5-dimethoxy-2-nitrophenyl)methanol copper(I) complex	350nm	NR	MeCN	NR	NR
				MeOH	0.0112	1.5%
				20mM HEPES buffer/ dioxane (1:1), pH 7.0	NR	NR
24.	53 , (4-(Bis(2-(2-(Ethylthio)ethyl)thio) ethyl)amino)phenyl)(4,5-dimethoxy-2-nitrophenyl)methanol mercury(II) complex	350nm	NR	MeCN	0.007	NR
				MeOH	NR	NR
				20 mM HEPES buffer/	NR	NR

		dioxane (1:1), pH 7.0				
25.	54 , (4-(Bis(2-((2-(Ethylthio)ethyl)thio)ethyl)amino)phenyl)(3-nitronaphthalen-2-yl) methanol silver(I) complex	350nm	NR	20 mM HEPES buffer/ dioxane (1:1), pH 7.0	NR	NR
26.	55 , Pyridine-2-carboxylic acid {1-(2-nitro-phenyl)-2-[(pyridine-2-ylmethyl)-carbamoyl]-ethyl)-amide) platinum(II) complex	320nm	NR	Phosphate buffer pH 7.4	NR	75%

*NR= Not Reported

Kaplan and his group first synthesized the light-activated ATP-caged molecule.¹³⁹ The caged-ATP molecule **26** remains intact until the light of the specific wavelength falls on it to release free ATP molecule (Figure 7). Calcium plays an important role in controlling the neurosynaptic transmission, hormone secretion and muscle contraction.¹⁴⁰ As shown in the Figure 8, the caged DM-nitrophen calcium complex ((1-(2-nitro-4, 5-dimethoxyphenyl)-N, N, N', N'-tetrakis [(oxycarbonyl)methyl]-1, 2-ethanediamine, **27**) was able to release the Ca(II) ion upon photo-irradiation. These calcium caged complexes were further used in various biological applications including muscle contraction and neurobiology.^{141,142} Later the next calcium caged complexes were designed to increase the photolysis efficiency.¹⁴³ The carboxylate rich chelator **27** was also used on other alkali metals like Sr(II), Ba(II), Mg(II) etc.¹³⁸ This concept of metal ion release is effective for many biological applications. The concept of calcium caged complexes created a roadmap for transition metals like copper, zinc and iron. K. J. Franz and group reported a copper(II) cage using nitrogen-rich bispyridylamide ligand (H₂cage) to form [Cu(OH₂)(cage)] (**30**) as first generation caged complex.¹³⁸ On photo-irradiation, **30** release the copper as shown in Figure 9. The complete photo-cleavage occurs within 4 min exposure to UV light with 160% formation of hydroxyl radicals. As the binding affinity of H₂cage for copper was not strong enough. The second generation ligands (imcage **31**, amcage **32**, 3arm-1 **33**, 3arm-3 **34**, macrocage **35**, ZnCleave-1 **36**, 1Gcage **37**) were synthesized.^{138,144} However, the binding affinities of Cu(II) were unfavorable for these ligands due to low chelating ability, electronic and steric effects. This ultimately led to development of a third-generation ligand (3Gcage). 3Gcage ((pyridine-2-carboxylic acid {1-(2-nitro-phenyl)-3-[(pyridin-2-ylmethyl)-amino]-propyl)-amide) demonstrated good binding affinity for Cu(II) until the activation of UV light cleaves the ligand backbone (Figure 10). Cu3G cage (**38**) was found to enhance the generation of hydroxyl radicals to 300% on light activation causing non-apoptotic cell death.^{144,145} [Cu(Coucage)] (**39**)¹⁴⁶ a Cu(II) complex of a tetradentate coumarin derived ligand shows fluorescence quenching in live MCF7 cells. Exposure to UV light cleaves the bond causing fluorescence 'turn-on' and restoring the fluorescence upto 67%. This strategy can be used effectively to study copper trafficking at cellular level. S. C. Burdette and co-workers reported CuCleave-1 (**40**) which established

binding and release of copper in +1 oxidation state on light-activation.¹⁴⁷

Further, a set of Zn(II) caged complexes were synthesized in order to study the Zn(II) ion signalling.¹⁴⁸⁻¹⁵⁴ S. C. Burdette reported three Zncast cages (**41**, **42** and **43**). Among these, **43** exhibits highest affinity for zinc.¹⁵⁵ [Zn(CrownCast)]²⁺ **44** was the first in the series with crown ether receptor that has capability to bind Zn(II) ion.¹⁴⁹ Upon photo-irradiation **44**, nitrosobenzophenone was formed as a photo-product which has affinity for Zn(II). ZnCleave-1 (**45**), ZnCleave-2 (**46**) and ZnDiCast (**47**) were synthesized as the next generation Zn(II) caged complexes^{150,151,156} with **45** exhibiting greater binding affinity than others.^{149,150,157} [Zn(NTAdeCage)] (**48**) was able to release Zn(II) ions upon photolysis in human *Xenopus laevis* oocytes. Intracellular distribution of [Zn(DPAdeCage)]²⁺ (**49**) on human dermal fibroblast (HDF) displayed enhanced fluorescence on activation of light.¹⁵⁴

Iron is important in life processes and ferritin and transferrin controls iron storage and trafficking within the cells.¹⁵⁸ Siderophores are naturally occurring unlockable cages with high affinity for Fe(III) ions. Marine siderophores called aquachelins are able to coordinate Fe(III) ion which in presence of UV light releases Fe(II) ions on cleavage of siderophore backbone.^{159,160} [Fe(FerriCast)Cl₂]⁺, **50**¹⁶¹ is non-siderophore Fe(III) photocaged complex. **50** on photo-irradiation weakens the binding affinity and releases Fe(III) ions. Unfortunately, **50** decomposes in aqueous medium limiting its application in biological systems. S. Burdette and group synthesized argencast photocaged ligand with acyclic polythioether 3, 6,12,15-tetrathia-9-azaheptadecane receptor and 4, 5-dimethoxy-2-nitrobenzyl/ naphthyl-based nitrobenzyl group.¹⁶² Binding affinities of argencast-1 revealed interaction with Ag(I), Cu(I) and Hg(II) metal ions (**51**, **52** and **53**). However, only Ag(I) was able to bind the argencast-1 in both organic and buffered environment. The photoreaction of argencast-1 converts the nitrobenzyl into nitrosobenzophenone that participates in a resonance interaction with a metal-bound aniline nitrogen atom. The structural change following photolysis decreases availability of the nitrogen lone pair for Ag(I) coordination, but strong interactions between Ag(I) and the thioether ligands mitigates the release of metal ion. Along with argencast-1, argencast-2 (**54**) was shown to bind Ag(I) in both organic and aqueous media with similar quantum efficiency.

The dose-limiting toxicity and non-selectivity of cisplatin between normal and cancer cells is a major drawback for treatment of cancer.¹⁶³ Delivery of drugs at the tumor site would minimize the toxicity to normal cells.¹⁶⁴ To enhance the selectivity of platinum to the target, Pt(II) was incorporated in the tetradentate ligand bearing a photolabile group, [Pt(cage)] (**55**).¹⁶⁵ This neutral platinum caged complex upon light activation converts to charged Pt(II) complex and induces photo-dependent cytotoxicity in MCF-7 cell line. Photophysical data and quantum efficiencies of all the photocaged complexes are compiled in table 1.

3. Para-nitroaromatic compounds as nitroreductase (NTR) active agents

The concept of 'bioreductive therapy' involves enzymatic reduction of non-toxic prodrug to reduced form which is more cytotoxic and therefore can be used effectively in cancer chemotherapy, solid tumor radiosensitization, and killing microorganisms.^{166,167} Nitroaromatic compounds such as nitrofurans, nitropyrenes, nitrobenzenes and several other nitro aryl compounds are known for their toxic, mutagenic and carcinogenic properties.¹⁶⁸ As described earlier large tumors contain very less amount of oxygen that creates highly reducing environment known as hypoxia. Decrease in oxygen level leads to increase in reductive enzymes such as nitroreductase (NTR), quinone reductase and azoreductase.

Among these, NTR is directly related to the amount of intracellular levels of hypoxia.¹⁶⁹⁻¹⁷¹ NTR is overexpressed in various tumors and plays an important role in tumor invasion, progression and angiogenesis.¹⁷² Therefore, NTR can be used as biomarker for evaluating the levels of hypoxia in tumor cells.^{171,172} NTR belongs to the family of flavin-containing enzymes which effectively reduces the nitro-aromatic groups to amines in presence electron donor such as nicotinamide adenine dinucleotide (NADH).^{173,174} The mechanism of flavin based enzyme is divided into two types as shown in Figure 11,^{175,176} Type I NTRs are oxygen insensitive and are capable of reducing nitro-aromatic compounds to hydroxylamine/amine in presence of O₂. Type II NTRs are oxygen sensitive and reduced when oxygen is absent. Type I NTR is present in most of the bacteria like *Escherichia coli*,^{177,178} *Helicobacter pylori*¹⁷⁹ and *Vibrio fischer*¹⁸⁰ including like ESKAPE family (*Enterococcus faecium*, *Staphylococcus aureus*, *Klebsiella pneumoniae*, *Acinetobacter baumannii*, *Pseudomonas aeruginosa*, and *Enterobacter* species)¹⁸¹⁻¹⁸³ and also can be used to activate drugs for the treatment of cancer.¹⁸⁴

The early work of Olive and Durand in 1980's demonstrated that nitroaryl compounds are well recognized as hypoxia selective agents.¹⁸⁵ Among the family of nitrofurans reported by them 3-((E)-2-(5-nitrofur-2-yl)vinyl)-1, 2, 4-

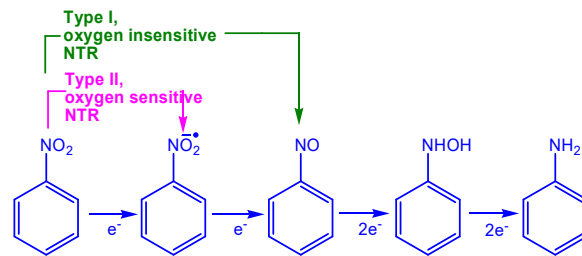


Figure 11. Mechanism of oxygen insensitive (type I) and oxygen sensitive (type II) nitroreductase on nitro-aromatic compound.¹⁸⁶

Nitro-furan and aryl derivatives		
 56	 57	 58
Nitro-imidazole derivatives		
 59	 60	
 61	 62	
2-Nitroimidazole-naphthalimide derivatives		
 63	 64	

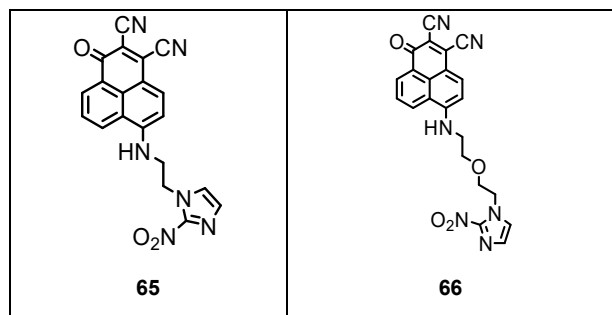


Figure 12. Structures of nitro-aryl conjugates used as probes for detection of hypoxia.

oxadiazol-5-amine (**56**) was found to be highly responsive for hypoxic cells (Figure 12).^{187–190} Further, a number of nitroaryl compounds in which 1-(2, 3-dimethoxy-6-nitroanthracen-9-ylamino)-3-(diethylamino) propan-2-ol (**57**) and nitronaphthalimide (**58**) were shown to be non-fluorescent unless they get completely reduced to respective amines which fluoresce at high intensity (Figure 12). However *in-vivo* studies revealed that **57** did not accumulate to a greater extent in solid tumors.¹⁸⁷

Later, Hodgkiss *et al*¹⁹⁰ synthesized a series of 2-nitroimidazole compounds bearing fluorophores such as naphthalimide (**59**), coumarin (**60**), indolizine (**61**) and bicyclic bimeane (**62**) as shown in the Figure 12. Bio-reduction of these moieties exhibited 5-17 fold increase in fluorescence when tested in V79 Chinese hamster cells. A series of 1, 8-naphthalimides with one or two 2-nitroimidazole moieties **63–66** displayed high fluorescence in V79 Chinese hamster hypoxic cells.^{191,192} Recently, X. Qian and his co-workers developed a first ratiometric fluorescent probe **67** (Figure 13a), capable of selective reduction in presence of NTR and NADH that changes its fluorescence from blue to green.¹⁷⁰ Similar response was also observed in A549 cells in hypoxic condition. In addition, **67** was found to be least toxic making it a potential candidate for hypoxia imaging.

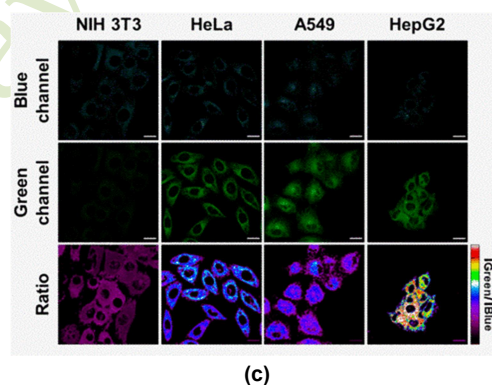
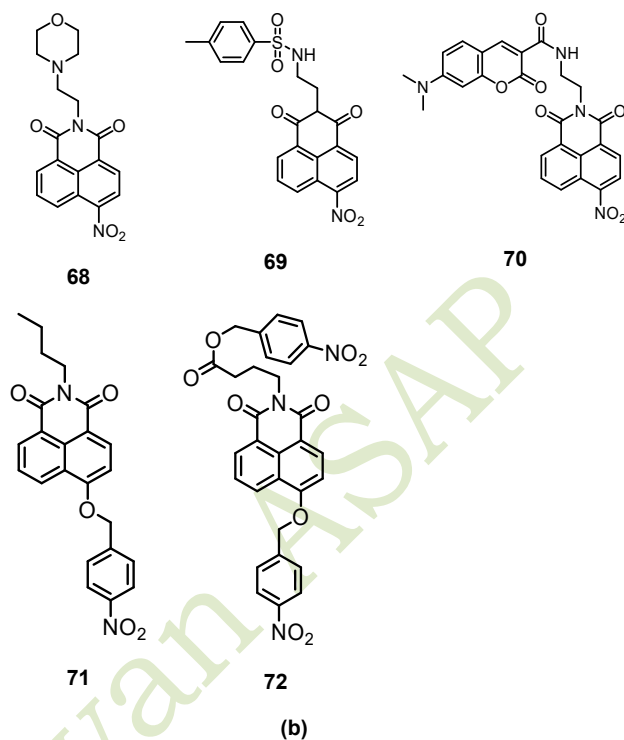
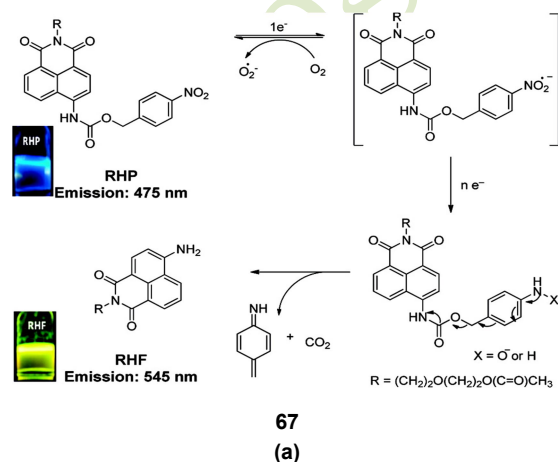


Figure 13. (a) Proposed detection mechanism of fluorescent probe **67**, Adapted from reference¹⁹³ (b) Chemical structures of naphthalimide-based fluorescent probes, (c) Confocal microscopy images of probe **70** (0.5 μ M) in noncancerous cells (NIH3T3) and various cancer cells (HeLa, A549, and HepG2). Adapted from reference¹⁹⁴.

H. Ma and group¹²² designed lysosome-targeting 'turn-on' probe for detecting lysosomal nitroreductase and hypoxia. The probe **68** was incorporated with morpholine as a lysosome-targeting unit with 4-nitro-1, 8-naphthalimide as a fluorochrome and specific substrate for NTR. This probe displayed capability of visualizing the change in lysosomal NTR in live A549 cells under hypoxic condition. These studies revealed that the level of NTR in lysosomes is less than that in the cytoplasm. W. Lin *et al*¹⁹⁵ reported probe **69** which was able to detect the NTR in endoplasmic reticulum (ER) in the cells. Here, the naphthalimide fluorophore was conjugated with methyl sulphonamide moiety. The presence of sulphonamide moiety is responsible for its selectivity to

ER of live HeLa cells. This probe showed strong fluorescence at 543 nm with high selectivity, sensitivity and low cytotoxicity to cancer cells.

M. H. Lee¹⁹⁴ designed self-calibrating dual emission fluorescent probe **70** by conjugating coumarin with nitronaphthalimide moiety that was successfully used in evaluating the NTR activity in noncancerous (NIH3T3), cancerous (HeLa, A549, and HepG2) and hypoxic cells. The emissions from coumarin (blue) and naphthalimide (green) moieties were considered as internal reference signal and NTR-responsive signal respectively. The green emission (505–600 nm) in HeLa, A549 and HepG2 cells was significantly enhanced compared to that of NIH3T3 cells whereas the blue emission (420–475 nm) was relatively unchanged (Figure 13c).

Next, S. Sun *et al.*¹⁹⁶ reported a small molecular weight fluorescent probe **71** consisting of 1, 8-naphthalimide fluorophore. The probe **71** exhibited high sensitivity, selectivity and low toxicity with a lower detection limit (3.4 ng/mL). Further, incubation of **71** with HepG-2 cells displayed intense emission which increased in a dose-dependent manner. This probe exhibited high selectivity and specificity towards NTR in bacteria (*E. coli* and *S. aureus*) and tumor cells (HL-7702, HepG-2 and MCF-7).

Q. Ye and group¹⁹⁷ synthesized two-photon fluorescent probe **72** which was activated in presence of NTR. When NP69 cells were incubated in presence of **72**, no fluorescence was detected under normoxic condition. However, gradual increase in the fluorescence signal was noted with decreasing oxygen concentration. Among various tumors, nasopharyngeal carcinoma (NPC) is the most common malignant tumor of the head and neck. **72** demonstrated better penetration through 100 μm thick NPC tissue with NTR detection. Further, the evaluated NTR activity revealed significant fluorescence enhancement in hypoxic HeLa cells. Probe **73** incorporates Nile Blue as a fluorophore for detection of NTR (Figure 14a) to improve the cell permeability of the probe.¹⁹⁸ It was found to be more selective and sensitive for NTR with detection limit 180 ng/mL. It was non-toxic to A549 cells and exhibited high fluorescence in hypoxic condition (Figure 14b). Similarly, probe **74**, was designed incorporating xanthene derivative, seminaphthorhodafluor (SNARF), with *p*-nitrobenzyl group attached to it through ether linkage.¹⁹⁹ Reduction of *p*-nitrobenzyl moiety by NTR releases fluorescent SNARF acting as a fluorescent pH probe (Figure 15).

Nowadays, near infrared (NIR) fluorescence probes (700–1000nm) are gaining a lot of preclinical and clinical applications due to their high spatial resolution, portability and real time display. NIR probes can penetrate through deep organic tissues (<1–2 cm depth) and reduce damage to neighboring cells and tissue. Hence probes that emit in NIR regions were designed (Figure 16) by H. Nagasawa *et al.*²⁰⁰ comprising a tricarbocyanine moiety as NIR fluorophore and two 2-nitroimidazole moieties as exogenous hypoxia markers **75**. The probe **75** when trapped in GPU-167 cancer

cells gave fluorescence emission at 778 nm. Similarly, X. Zhang *et al.*,²⁰¹ designed another cyanine based fluorophore which was able to emit at 708 nm. Here the probe **76** was introduced with sulphonate groups to make enhance its water solubility for biological applications and to prevent its aggregation. F. Xu *et al.* synthesized probe **77** semi-cyanine fluorophore by linking *p*-nitrophenyl group via alkenyl linker. This probe was able to detect the normoxic and hypoxic conditions in A549 cells.²⁰² Y. Sha and coworkers designed probe **78** by using 2, 3, 3-trimethyl-3H-benzof[*h*]indolinium and a *p*-nitrobenzyl moiety as NTR sensor. Further the NTR activity was studied on HeLa cells. The enhancement of fluorescence signal at 720 nm was noted in hypoxic environment²⁰³. Similarly, H. Ma and group¹⁷³ synthesized hemicyanine **79** from the unstable cyanine precursors. This probe possessed NIR spectroscopic feature with higher stability and was able to visualize the distribution of NTR in live zebrafish.

Another cyanine dye **80** was able to image the mammalian mitochondria¹⁷⁶ in live A549 cells. To enhance the lipophilicity of cyanine probe, nitroaromatic moiety was introduced while designing the probe **81**.²⁰⁴ This probe showed high specificity, sensitivity and rapid response to NTR over other biological analytes. This probe successfully monitored intracellular NTR in real-time by imaging live bacterial cells (*Escherichia coli*, *Staphylococcus aureus*, *Klebsiella pneumoniae*, methicillin-resistant *Staphylococcus aureus* (MRSA)). L. Chen *et al.*²⁰⁵ developed cyanine 'turn-on' probe **82** for quantitative detection of NTR in A549 cells and cisplatin resistant A549 (A549/DDP) xenograft nude mice. Later, J. Ge *et al.*¹⁷⁴ reported first single fluorescent chemodosimeter, **83** that could simultaneously detect NTR in mitochondria and lysosome in live HeLa cells, containing aromatic azonia and benzo[e]indol anion skeleton.

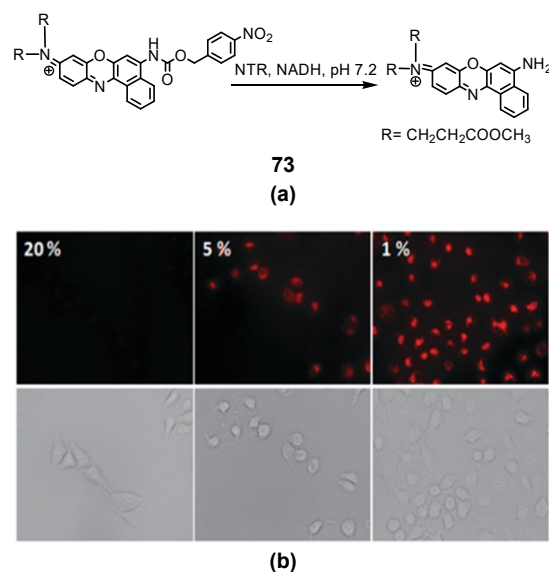


Figure 14. (a) Reaction mechanism of **73**. (b) Fluorescence images of A549 cells incubated in normoxic condition ($p\text{O}_2$ 20%) and in hypoxic condition ($p\text{O}_2$ 5% and 1%). Adapted from reference¹⁹⁸.

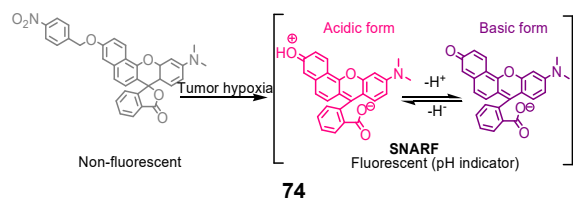


Figure 15. Bio-reduction of non-fluorescent (**74**) to release pH responsive fluorophore SNARF. Adapted from reference¹⁹⁹.

X. Ma and group²⁰⁶ reported a near infrared fluorescent probe (**84**) for sensing bacterial NTRs. This probe exhibited 'drug-like' ClogP with good biocompatibility. The probe was able to monitor the NTR activity (*in-vivo* and *in-vitro*) and image the bacteria at 720 nm. The quantum yield of **84** was 0.004 and 0.041 before and after the enzymatic reaction respectively. Furthermore, the homologous NTRs were profiled visually for various bacterial species including anaerobic bacteria (*B. fragilis*, *B. thetaiotaomicron*, and *B. bifidum*) and aerobic bacteria (*Pseudomonas aeruginosa*, *E. coli* 0377, *Bacillus cereus*, *Staphylococcus hominis*, *E. faecalis*, *E. coli* 3079, and *Klebsiella pneumoniae*) along with rapid protein identification.

H. Hu *et al*²⁰⁷ developed bacteria-specific neomycin-based stable, water-soluble fluorogenic probe **85** for fast measurements which displayed excellent selectivity toward NTR. The probe sensed intracellular basal NTR activity in live bacteria both *in vitro* and *in vivo*. Sulphonate ester linked electron-withdrawing nitro group could efficiently bring the fluorescence quenching through photoinduced electron transfer (PET). *In-vivo* studies were carried out on Gram-positive bacterial strain *Staphylococcus aureus* (*S. aureus*, ATCC 29213) as well as the Gram-negative bacterial strain *Enterobacter cloacae* (*E. cloacae*, ATCC 13047) with or without NTR inhibitor (dicoumarin). The probe **85** on treatment with bacterial cell in concentration-dependent manner increases the fluorescence signal at 803 nm. Co-incubation with the NTR-inhibitor significantly reduced the fluorescence signal in bacterial infections. It was successfully applied for non-invasive detection of NTR from bacterial and cancer cells simultaneously in mice bearing CT26 tumor infected with *S. aureus*.

Further, J. Yu and group²⁰⁸ synthesized two trimethincyanine probe incorporating *para*- and *meta*-nitrophenyl moieties at polymethine chain. The probe with *para*-nitrophenyl group, **86**, gave positive recognition of NTR. This probe showed rapid, good sensitivity and negligible cytotoxicity toward the hypoxic A549 cells with enhanced fluorescence signal due to reduction of *para*-nitrophenyl group. Additionally, the enzymatic steady-state kinetic analysis, molecular docking and molecular dynamic simulation were also evaluated. The simulation studies evidenced the close contact between the nitro group in **86** and the active center of cofactor NTR. The matching of hydrophobic center of nitrophenyl group and the binding pocket near the cofactor of NTR facilitated the binding and catalytic reaction between probe and NTR. The catalytic efficiency (k_{cat}/K_m) of **86** was maximum at 10.85 $\mu\text{M}/\text{s}$.

An ultrasensitive near infrared probe **87** by Y. Gu *et al*,²⁰⁹ was able to detect *in-vivo* hypoxic condition in deep tissues by responding to NTR. The probe **87** showed fast response and prolonged imaging time in the tumor-bearing mice. Additionally, **87** demonstrated accurate and timely imaging of ischemic liver and enteritis sites in mice. The probe also showed good permeability while continuously imaging hypoxic cells (HepG2 cells).

A. Jayagopal *et al* developed two hypoxia sensitive probes **88** and **89** employing fluorescein as a reporting molecule. **89** exhibited 32-fold fluorescence enhancement in hypoxic retinal cells than normoxic retinal cells at concentration as low as 10 μM .²¹⁰ Hypoxia-sensitive theranostic probe **90** comprising biotinylated rhodol in conjunction with *p*-nitrobenzyl group via carbonate linker was reported by S. Bhuniya and coworkers²¹¹. This probe was stable within the biological range of pH 6-8. The probe **90** was selective towards NTR in liver microsomes and nematode (*Caenorhabditis elegans*). M. P. Landry *et al*²¹² described highly sensitive NTR responsive three fluorescein probe designed with *para*-, *meta*- or *ortho*-nitrobenzyl groups. Among these, the probe with *p*-nitrobenzyl group **91** exhibited highest fluorescence quantum efficiency, extinction coefficient (around 490 nm) and water solubility under physiological conditions. Confocal fluorescence imaging and flow cytometry confirmed uptake of **91** by HepG-2, A549, and SKOV-3 with significant fluorescence enhancement under reducing conditions. In addition, **91** could distinguish different growth stages of tumors from the degree of hypoxia in tumor in mice models. D. Chang and group²¹³ designed NTR-responsive fluorescent probes with *o*-methyl fluorescein and *o*-methyl rhodol fluorophores. Here the *p*-nitrobenzyl moiety was linked with fluorophore via ether (**92**), carbonate (**93**), secondary amine (**94**), tertiary amine (**95**) and carbamate (**96**) linkers. Here the effect of linkages with fluorophore was studied using different spectroscopic techniques, temperature, pH stability, kinetics and concentration-dependency with NTR reactions. It was found that probes with ether and carbamate linkers presented better biocompatibility, high sensitivity (below 1 μM) and strong fluorescence response with NTR. From imaging studies, **92** and **96** were found to be putative hypoxia markers in live cells.

Along with fluorescein fluorophores researchers also developed rhodamine-based probes for detection of NTR (Figure 17). C. Wang and his group²¹⁴ designed rhodamine probe **97** in one-step synthesis. Probe **97** showed 110-fold increase in fluorescence intensity when applied to monitor NTR production during *E. coli* growth. It was also able to visualize NTR production in malignant C-27 oral cancer cells under hypoxia. Similarly, G. Jaun *et al*²¹⁵ developed rhodamine derived probes (R6G) by linking *ortho*-, *meta*- and *para*-nitrobenzyl moiety via hydrazide linker. Among them the probe with *para*-nitrobenzyl moiety **98** was able to detect NTR in physiological pH in HeLa cells with least toxicity and increase in fluorescence signal. H. Ma and group²¹⁶ synthesized a newly developed fluorescent probe which was able to detect NTR and ATP (adenosine triphosphate) in hypoxic condition. The hybrid probe **99** was

designed by combining two fluorophores rhodamine and 1, 8 naphthalimide via diethylenetriamine linker. This probe was able to monitor NTR and ATP in hypoxic and normoxic

conditions in HeLa cells. The detection limit of **99** for ATP was found to be 0.05 mM.

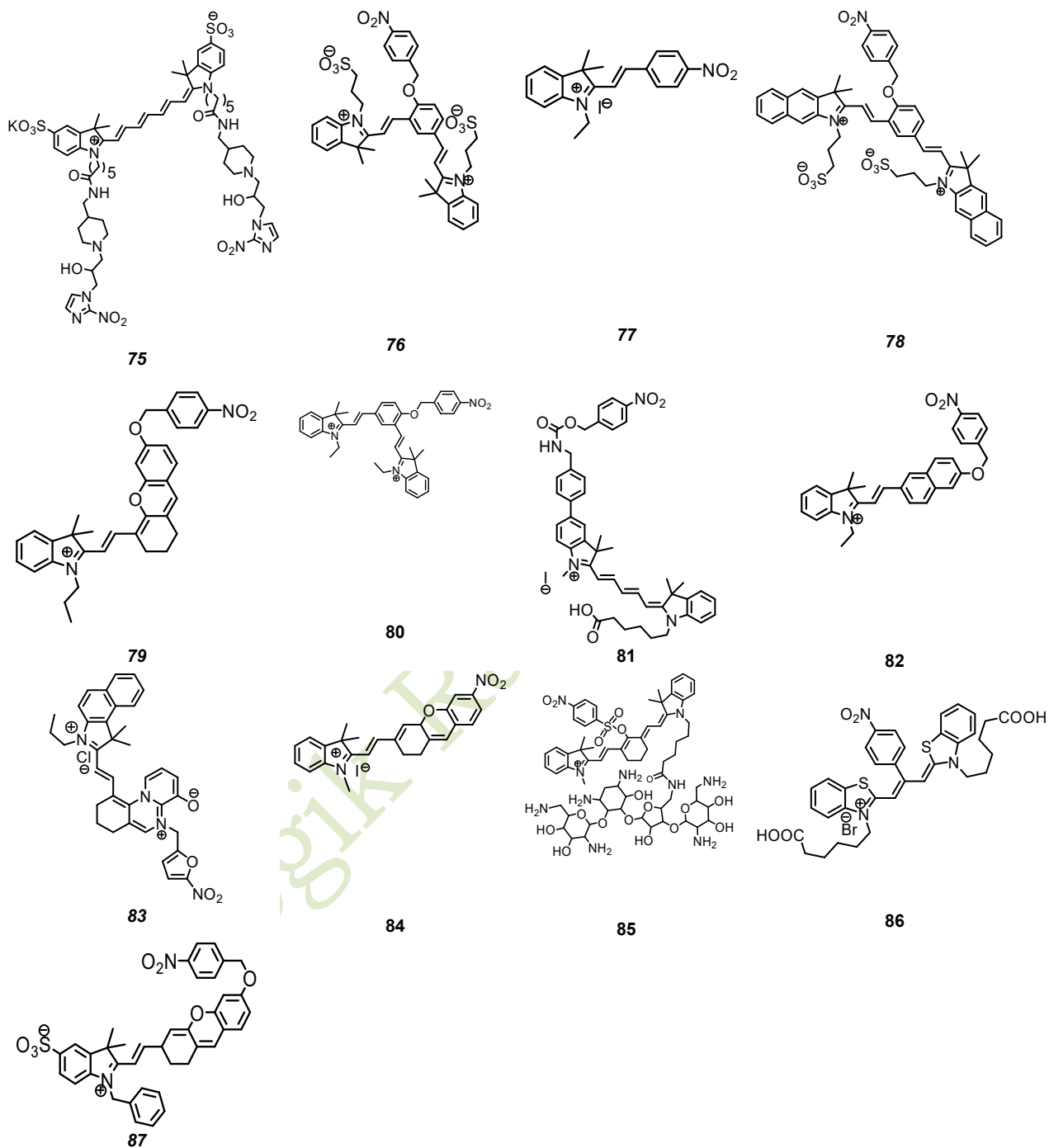


Figure 16. Cyanine-based dyes for NTR-responsive probes.

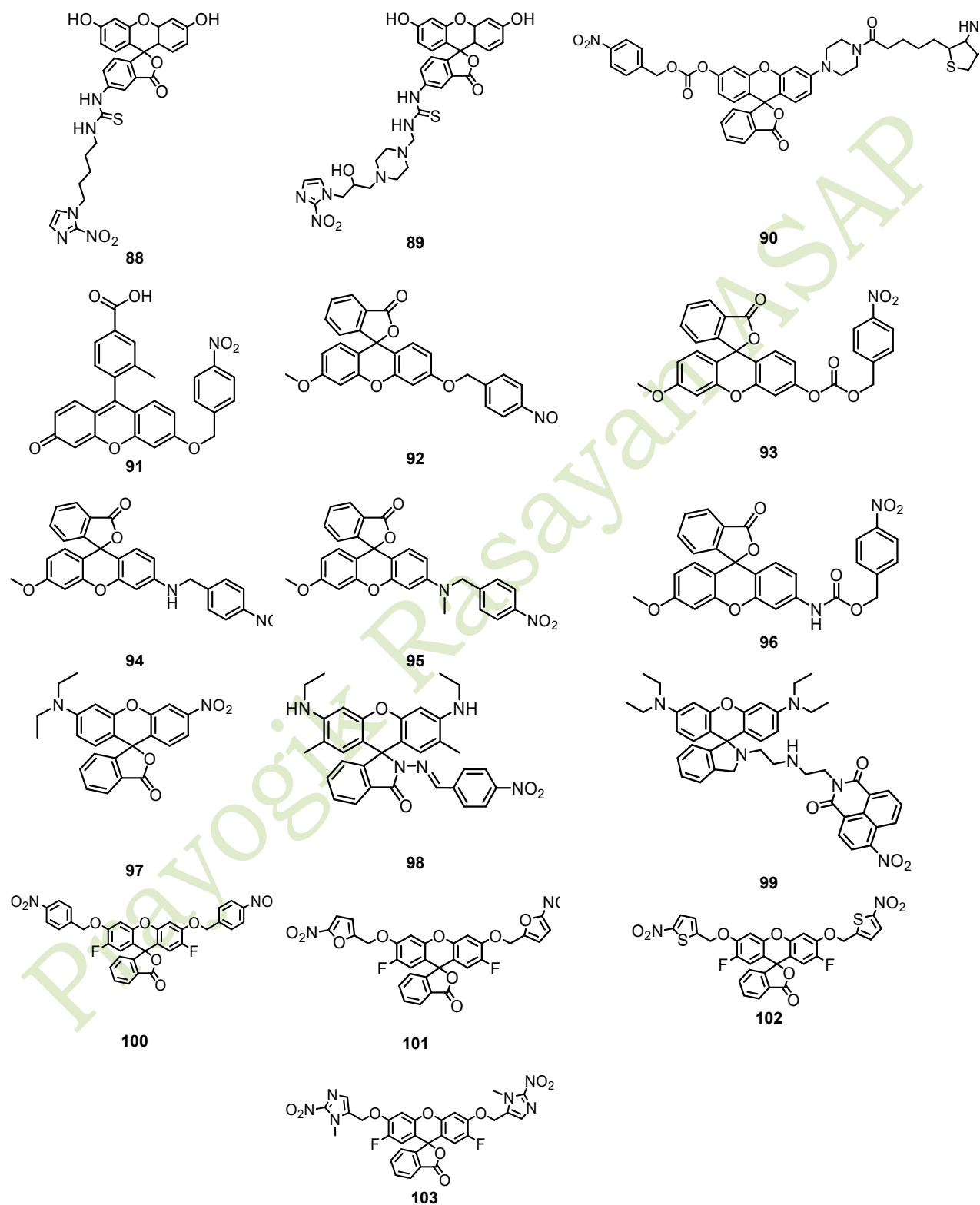


Figure 17. Fluorescein-based NTR responsive probes

L. D. Levis and group²¹⁷ synthesized a series of four fluorogenic probes (**100-103**) based on 2', 7'-difluorofluorescein (Oregon Green). These probes on alkylation with phenolic oxygen locks the molecule in non-fluorescent lactone form resulting in weak fluorescence signal. On testing these probes it was found that probe **103** with bis(2-nitro-N-methyl imidazolyl) moiety showed significant enzymatic activity in presence of endogenous intracellular reducing environment in mammalian cells. The k_{cat}/K_M value of **103** was found to be $8.1 \pm 0.8 \times 10^4 \text{ M}^{-1} \text{ s}^{-1}$. However, the probes with bis(5-nitrofuranyl) (**101**) and bis(5-nitrothiophenyl) (**102**) Oregon Green showed very low reactivity with k_{cat}/K_M value $3.0 \pm 0.5 \times 10^3 \text{ M}^{-1} \text{ s}^{-1}$ and $\sim 6 \times 10^2 \text{ M}^{-1} \text{ s}^{-1}$ respectively. In contrast bis(nitrobenzyl) compound (**100**) was largely unreactive.

Along with fluorescein and rhodamine, BODIPY (boron dipyrromethene) based fluorophores are also being developed due to its excellent photostability, high quantum yield, and sharp absorption and emission bands (Figure 18). Due to high lipophilicity BODIPY probes tend to cross the cellular membrane and accumulate in subcellular membranes.²¹⁸ BODIPY (4, 4-difluorouoro-4-bora-3a, 4-diaza-s-indacene) exhibits excellent photochemical stability, low biological toxicity, high quantum yield and high extinction coefficient.²¹⁹⁻²²² S. Shao *et al* developed the probe **104** where a probe incorporating BODIPY moiety attached to 5-nitrofurane as a substrate for NTR.²²³ Quaternized pyridine moiety was introduced for good water solubility.²²⁴⁻²³⁰ NTR-catalyzed reduction of **104** releases free 4-pyridinyl-substituted BODIPY giving 20-fold increase in fluorescence intensity. Further, this probe was able to track quantitatively the amount of NTR produced in *E. coli* in time-dependent manner. Another BODIPY based probe, 3-(4-hydroxy-3-nitro styryl)-BODIPY (**105**), involving a styryl substituent with -OH and -NO₂ groups exhibited fluorescence 'Turn-on' under hypoxia.²³¹ Using a water-soluble BODIPY-based chemodosimeter **106**, Y. A. Volkova²³² successfully imaged hypoxia status in human non-small-cell lung cancer A549 cells. Here the probe was incorporated with two N-alkylpiperidinyl groups for enhancing both its water solubility and cellular uptake.

Another probe meso-ester-1, 3, 5, 7-tetramethyl- BODIPY (**107**), employing BODIPY was developed by Y. Kim *et al*.²³³ Reduction of **107** in presence of NTR produced meso-carboxylate-BODIPY with ~ 220 -fold fluorescence enhancement. C. Zhao and group reported mitochondria-targeted fluorophore probe appended with *p*-nitrobenzyl thioether and triphenylphosphine functionalities to the parent BODIPY, **108**.²³⁴ In presence of enzyme nitroreductase, **108** was able to undergo 1, 6-elimination reaction that releases fluorophore emitting in the near infrared region.

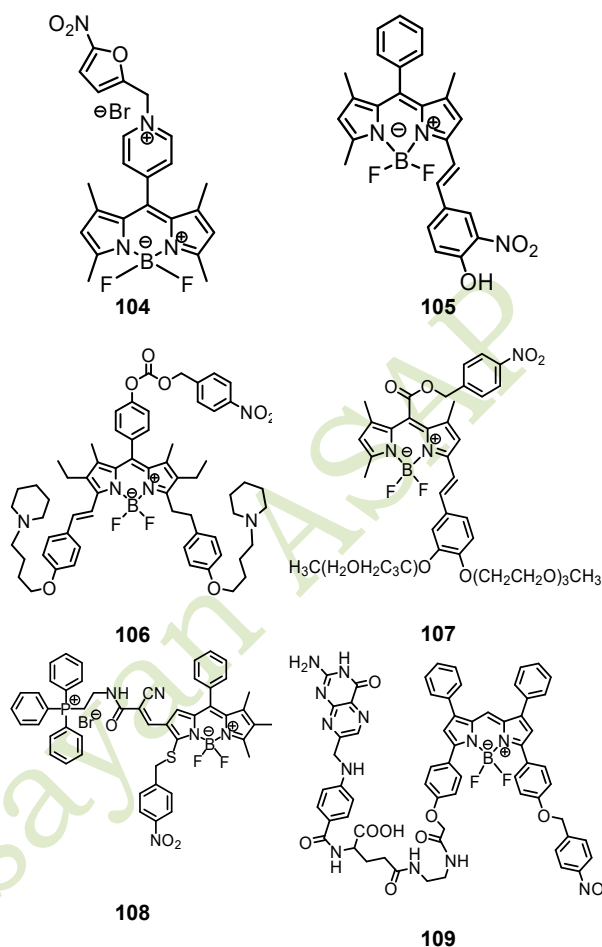


Figure 18. Conjugates of BODIPY-based hypoxia active probes.

This probe demonstrated selective detection of nitroreductase in mitochondria.²³⁴ Another BODIPY-based NTR triggered molecule emitting in near infrared region was designed by Jonathan L. Sessler and his coworkers.²³⁵ The molecule **109** was conjugated with folate due to which it is easily taken up folate receptor-positive CT26 cancer cells. This makes **109** a useful cancer-targeting agent.

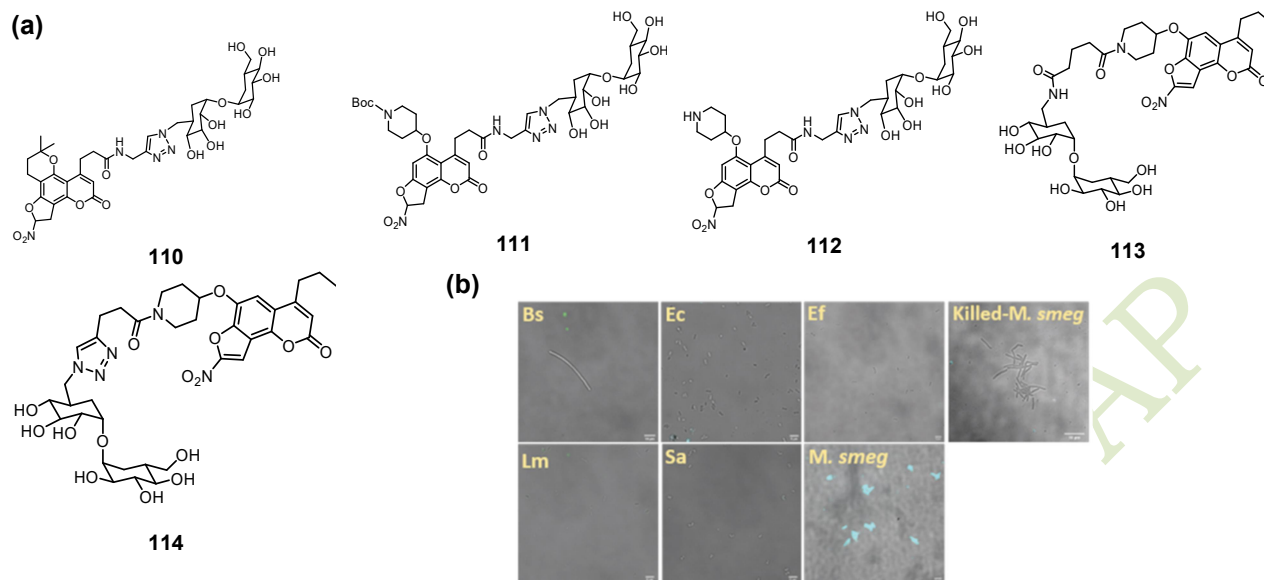


Figure 19. (a) Nitrofuranyl calanolides conjugates for detection of NTR in mycobacteria, (b) Overlap imaging (bright-field and cyan fluorescence) of *Bacillus subtilis* (Bs), *Escherichia coli* (Ec), *Enterococcus faecalis* (Ef), *Listeria monocytogenes* (Lm), *Staphylococcus aureus* (Sa), *Mycobacterium smegmatis* (M. smeg), and heat-killed *Mycobacterium smegmatis* (killed-M. smeg) cells incubated with 100 μ M **124** for 1 h.

A novel set of nitrofuranyl calanolides conjugated with trehalose (**110-114**), for detection of NTR Rv2466c in *Mycobacterium tuberculosis* (*Mtb*) (Figure 19a) was designed by G. Liu and group.²³⁶ Determining the location of *Mtb* in host cells is of great importance for understanding how the pathogens survive and protect themselves under the host pressure. Nitrofuranyl calanolides were found to kill both replicating-*Mtb* (R-*Mtb*) and nonreplicating-*Mtb* (NR-*Mtb*). Among the set of nitrofuranyl calanolides, probe **114** was able to rapidly detect single cells of *Mtb* under different states via the Rv2466c mediated reductive mechanism. Investigations on different bacteria, viz. *B. subtilis*, *E. coli*, *E. faecalis*, *Listeria monocytogenes*, *S. aureus* including *M. smegmatis* and heat killed *M. smegmatis* revealed that probe **114** selectively detected live *M. smegmatis* (Figure 19b). Additionally, the probe **114** could detect *Mtb* within macrophages and in sputum samples from TB patients.

So far, only few metal complexes employing this strategy are developed (Figure 20), Gd(III)-Dotarem *para*-nitrobenzyl complex (**115**) was designed to enhance MRI contrast in presence of enzyme NTR as Gd(III) is MRI active element and was conveniently used for detection of NTR in live *E. coli* cells.²³⁷ This is the first MRI agent for monitoring NTR in live bacteria. Nitroimidazole-ruthenium conjugate ([Ru(dip)₂(bpy-2-nitroimidazole)]Cl₂ (**116**) is Ru(II) complex that gets retained selectively in hypoxic cells.²³⁸ The probe **116** was quite toxic to A549 cell line (LD₅₀ = 13 \pm 3 μ M) which was further decreased upto LD₅₀ = 7.7 \pm 4 μ M in hypoxic condition (1% oxygen). This was due to higher accumulation of **116** in hypoxic environment inside cells after 4 h of incubation.

The toxicity of **116** may also arise because of its interaction with the DNA.²³⁹ First lanthanide-based 'turn-on' luminescent probe **117**, reported by Marc Nazaré¹⁸¹ contains Tb(III) with sensitizing carbostyryl antenna that results in energy transfer to the Tb(III) after coming in contact with NTR. Laporte-forbidden f-f transitions of Tb(III) results in low extinction coefficient and effective excitation, thus enabling the energy transfer of the lanthanide from organic chromophore.²⁴⁰ This probe was capable of selectively sensing live bacteria which are highly multi-resistant pathogens of the ESKAPE family and are responsible for majority hospital infections. Similarly, K. S. Hong and group²⁴¹ designed lanthanide-based NTR probe **118** by encapsulating europium in DOTA bearing a 3-nitrothalamide group. This probe was able to detect the hypoxia in cellular levels via optical imaging of live *E. coli* cells, as well as *in-vitro* CEST (chemical exchange saturation transfer) MRI studies involving CT26 cancer cells. **118** was found to be appropriate for *in-vivo* monitoring of hypoxic regions in a CT26 mouse xenograft via the production of both an NTR-specific luminescence signal and CEST MRI imaging due to Intramolecular charge transfer (ICT) from the resulting free NH₂ functionality to Eu(III) ion. The photophysical and enzymatic rate values of all the fluorogenic probes and detection limits are given in the table 2.

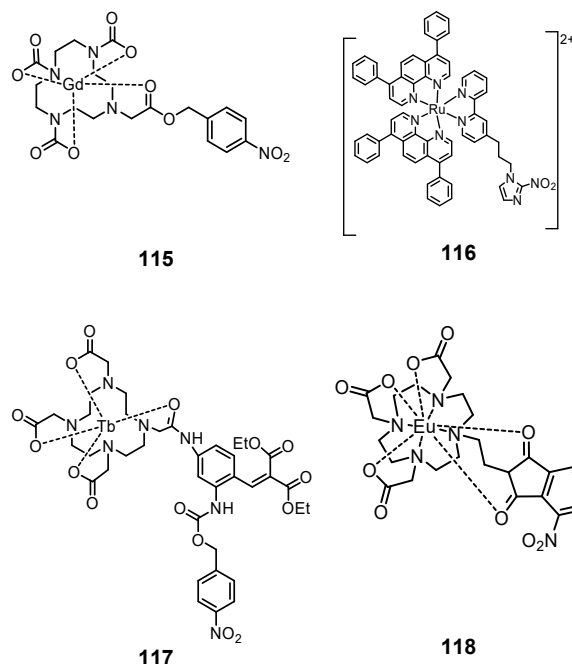


Figure 20. Metal complexes based NTR probes.

4. Conclusions

In this review, the development of non-platinum complexes as antiproliferative agents to stimulus-responsive molecules for targeted therapy is elaborated. The review gives an overview of molecules which can be used in future as anticancer agents with small modifications. It is interesting to learn how changes in cellular pH or amount of oxygen can modulate emission properties that can be used to develop sensing of tumor cell activity.

5. Acknowledgements

DUK acknowledges Savitribai Phule Pune University (SPPU) for fellowship and AAK acknowledges SPPU-RUSA-II funding (CBS:Th2.2), for financial support.

Table 2 Photophysical and enzymatic reaction rate values of NTR-responsive molecules.

Sr. No	Compound, chemical name	$\lambda_{ex/em}$, solvent	K_m	V_{max}	Detection limit
1.	67 , 2-(2-(6-nitro-1,3-dioxo-1H-benzo[de]isoquinolin-2(3H)-yl) ethoxy) ethyl acetate	410/550nm, 10mM PBS buffer (1% DMSO)	NR	NR	NR
2.	68 , 2-(2-morpholinoethyl)-6-nitro-1H-benzo[de]isoquinoline-1,3(2H)-dione	425/543nm, PBS buffer	45.6 μ M	0.062 μ M/s	2.2 ng/mL
3.	69 , 4-methyl-N-(2-(6-nitro-1,3-dioxo-1H-benzo[de]isoquinolin-2(3H)-yl)ethyl) benzenesulfonamide	440/543nm, 10mM PBS buffer (pH 7.4, 5% DMSO)	NR	NR	36 ng/mL
4.	70 , 2-(2-((1-(6-isopropyl-3-methylene-3,4-dihydronaphthalen-2-yl)vinyl) amino) ethyl)-6-nitro-1H-benzo[de]isoquinoline-1, 3(2H)-dione	430/550nm, 10mM PBS (pH 7.4, 10% DMSO)	23.4 μ M	3.42 μ M/s	0.733 ng/mL
5.	71 , 2-butyl-6-((4-nitrobenzyl)oxy)-1H-benzo[de]isoquinoline-1,3(2H)-dione	420/489nm, PBS buffer DMSO/H ₂ O (v/v 1:19, pH 7.0)	NR	NR	3.4 ng/mL
6.	72 , 4-nitrobenzyl 4-(6-((4-nitrobenzyl)oxy)-1,3-dioxo-1H-benzo[de]isoquinolin-2(3H)-yl)butanoate	450/560nm 10mM PBS buffer, (v/v DMSO pH 7.4	53.19 μ M	0.070 μ M/s	2.3 ng/mL
7.	73 , 3-methoxy-N-(3-methoxy-3-oxopropyl)-N-(5-((4-nitrobenzyloxy) carbonylamino)-9H-benzo[a]phenoxazin-9-ylidene)-3-oxopropan-1-aminium	658/580nm, 10mM PBS buffer (pH 7.4, 1% DMSO)	NR	NR	180 ng/mL
8.	74 , 10-(dimethylamino)-3-[[4-(nitrophenyl)methoxy]-spiro-[7H benzo[c] xanthene-7, 10 (30H)-isobenzofuran]-30-one	534/584nm, 10mM acetate (buffer pH 5.0)	NR	NR	NR
9.	75 , potassium 2-((1 <i>E</i> ,3 <i>E</i> ,5 <i>E</i>)-7-((<i>E</i>)-1-(7-(1-(1-hydroxy-2-(2-nitro-1H-imidazol-1-yl)ethyl)piperidin-4-yl)-5-oxoheptyl)-3,3-dimethyl-5-sulfonatoindolin-2-ylidene)hepta-1,3,5-trien-1-yl)-1-(5-(((1-(1-hydroxy-2-(2-nitro-1H-imidazol-1-yl)ethyl)piperidin-4-yl)methyl)amino)-5-oxopentyl)-3,3-dimethyl-3H-indol-	753/778nm, MeOH	NR	NR	NR

	1-ium-5-sulfonate				
10.	76 , 3, 3'-(((1E, 1'E)-4-((4-nitrobenzyl)oxy)-1, 3-phenylene) bis(ethene-2, 1-diyl)) bis(3, 3-dimethyl-3H-indole-1-ium-2, 1-diyl)) bis(propane-1-sulfonate)	590/708nm, 50mM PBS buffer (pH 7.4)	301.8 μ M	7.45 μ M/s	NR
11.	77 , (E)-1-ethyl-3,3-dimethyl-2-(3-nitrostyryl)-3H-indol-1-ium	490/556nm, 10 mM PBS buffer(pH7.0,1% DMSO)	NR	NR	40 ng/mL
12.	78 , 3, 3'-(((1E, 1'E)-4-((4-nitrobenzyl)oxy)-1, 3-phenylene) bis(ethene-2, 1-diyl)) bis(3,3-dimethyl-3H-benzo[f]indole-1-ium-2, 1-diyl))bis(propane-1-sulfonate)	605/720nm, 50 mM PBS buffer (pH 7.4)	18.28 μ M	0.03 μ M/s	NR
13.	79 , (E)-1-ethyl-3, 3-dimethyl-2- (2-(6-((4-nitrobenzyl)oxy)-2, 3-dihydro-1H-xanthen-4-yl) vinyl)-3H-indol-1-ium	670/705nm, 50 mM PBS buffer (pH 7.4)	32.2 μ M	3.7 μ M/s	14 ng/mL
14.	80 , 1-ethyl-2-((E)-3-((E)-2-(1-ethyl-3H-indol-1-ium-2-yl)vinyl)-4-((4-nitrobenzyl)oxy)styryl)-3,3-dimethyl-3H-indol-1-ium	572/703nm, 0.025mM PBS buffer(pH 7.4)	NR	NR	NR
15.	81 , 6-((E)-3, 3-dimethyl-2-((2E, 4E)-5-(1, 3, 3-trimethyl-5-(4-(((4-nitrobenzyl)oxy)carbonyl)amino) methyl) phenyl)-3H-1 λ ⁴ -indol-2-yl)penta-2,4-dien-1-ylidene)indolin-1-yl) hexanoic acid	620/657nm, 50mM Tris buffer (pH7.0,1.5% DMSO)	NR	NR	32.9 ng/mL
16.	82 , (E)-1-ethyl-3, 3-dimethyl-2-(2-(6-((4-nitrobenzyl)oxy) naphthalen-2-yl)vinyl)-3H-indol-1-ium	450/580nm, 10mM HEPES buffer (pH 7.4)	46.82 μ M	0.13 μ M/s	26 ng/mL
17.	83 , (E)-10-(2-(1, 1-dimethyl-3-propyl-1H-benzo[e]indol-3-ium-2-yl) vinyl)-5-((5-nitrofur-2-yl) methoxy)-8, 9-dihydro-7H-pyrido[1, 2-a]quinazolin-5-ium-3-olate	565/655nm, 10mM PBS buffer (pH7.4,5% DMSO)	NR	NR	3.2 ng/mL
18.	84 , 2-((E)-2-((Z)-3-(2-((Z)-1-(7-(((3-(3-amino-6-(aminomethyl)-4,5-dihydroxytetrahydro-2H-pyran-2-yl)oxy)-5-((3,5-diamino-2-((3-amino-6-(aminomethyl)-4,5-dihydroxytetrahydro-2H-pyran-2-yl)oxy)-6-hydroxycyclohexyl)oxy)-4-hydroxytetrahydrofuran-2-yl)methyl)amino)-7-oxoheptyl)-3,3-dimethylindolin-2-ylidene)ethylidene)-2-(((4-nitrophenyl)sulfonyl)oxy)cyclohex-1-en-1-yl)vinyl)-1,3,3-trimethyl-3H-indol-1-ium	700/801nm, 50 mM Tris-buffered saline (Tris/HCl, 1.5% DMSO, pH 7.4)	11.88 μ M	0.178 μ M/s	0.67 ng/mL
19.	85 , (E)-1,3,3-trimethyl-2-(2-(6-nitro-2,4a-dihydro-1H-xanthen-3-yl)vinyl)-3H-indol-1-ium iodide	670/720nm Phosphate solution	17.87 μ M	387.2 nM/min/mg	0.4 ng
20.	86 , 3-(5-carboxypentyl)-2-((1Z,3Z)-3-(3-(5-carboxypentyl)benzo[d]thiazol-2(3H)-ylidene)-2-(4-nitrophenyl)prop-1-en-1-yl)benzo[d]thiazol-3-ium bromide	550/570nm PBS buffer	0.1271 μ M	0.2872 μ M/s	0.117 μ g/mL
21.	87 , (E)-1-benzyl-3,3-dimethyl-2-(2-(6-((4-nitrobenzyl)oxy)-2,3-dihydro-1H-xanthen-3-yl)vinyl)-3H-indol-1-ium-5-sulfonate	650/710nm 5mM PBS buffer (1.0% DMSO, pH 7.4)	NR	NR	13.441 ng/mL
22.	88 , 1-(3', 6'-dihydroxy-3-oxo-4a',9a'-dihydro-3H-spiro[isobenzofuran-1,9'-xanthen]-5-yl)-3-(5-(2-nitro-1H imidazol-1-yl) pentyl) thiourea	490/520nm	NR	NR	NR
23.	89 , 1-(3', 6'-dihydroxy-3-oxo-4a', 9a'-dihydro-3H-spiro[isobenzofuran-1,9'-xanthen]-5-yl)-3-((4-(2-hydroxy-3-(2-nitro-1H-imidazol-1-yl)propyl)piperazin-1-yl)methyl) thiourea,	490/520nm	NR	NR	NR
24.	90 , 4-(5-(4-(3'-(3-(4-nitrophenyl)-2-oxopropyl)-3-oxo-3H-spiro[isobenzofuran-1,9'-xanthen]-6'-yl)piperazin-1-yl)-5-oxopentyl)tetrahydro-1H-thieno[3,4-d]imidazol-2(3H)-one	510/550nm, 10 mM PBS buffer (pH7.4,1% DMSO)	NR	NR	51.5 ng/mL
25.	91 , 3-methyl-4-(6-((4-nitrobenzyl)oxy)-3-oxo-3H-xanthen-9-yl)benzoic acid	490/515nm, 50mM Tris-buffered	NR	NR	0.66 ng/mL

		saline (pH7.4, 2.5% DMSO)			
26.	92 , 3'-methoxy-6'-((4-nitrobenzyl)oxy)-3 <i>H</i> -spiro[isobenzofuran-1,9'-xanthen]-3-one	454/520nm, 10mM PBS buffer (pH 7.4)	NR	NR	NR
27.	93 , 3'-methoxy-3-oxo-3 <i>H</i> -spiro[isobenzofuran-1,9'-xanthen]-6'-yl (4-nitrobenzyl) carbonate	454/520nm, 10mM PBS buffer (pH 7.4)	NR	NR	NR
28.	94 , 3'-methoxy-6'-((4-nitrobenzyl)amino)-3 <i>H</i> -spiro[isobenzofuran-1,9'-xanthen]-3-one	476/516nm, 10mM PBS buffer (pH 7.4)	NR	NR	NR
29.	95 , 3'-methoxy-6'-(methyl(4-nitrobenzyl)amino)-3 <i>H</i> -spiro[isobenzofuran-1,9'-xanthen]-3-one	490/536nm, 10mM PBS buffer (pH 7.4)	NR	NR	NR
30.	96 , 4-nitrobenzyl (3'-methoxy-3-oxo-3 <i>H</i> -spiro[isobenzofuran-1,9'-xanthen]-6'-yl)carbamate	476/516nm, 10mM PBS buffer (pH 7.4)	NR	NR	NR
31.	97 , 3'-(diethylamino)-6'-nitro-3 <i>H</i> spiro[isobenzofuran-1,9'-xanthen]-3-one	500/560nm, 10mM PBS buffer	NR	NR	0.6 ng/mL
32.	98 ,3',6'-bis(ethylamino)-2'-methyl-2-((4-nitrobenzylidene)amino)spiro[isindoline-1,9'-xanthen]-3-one	500/557nm, PBS buffer (pH 7.0)	NR	NR	14.3 ng/mL
33.	99 , 3',6'-bis(diethylamino)-2-(2-((2-(6-nitro-1 <i>H</i> -benzo[<i>de</i>]isoquinolin-2(3 <i>H</i>)-yl)ethyl) amino)ethyl)spiro[isindoline-1,9'-xanthen]-3-one	540/580nm, 10 mM Tris buffer (pH 7.4)	NR	NR	120 ng/mL
34.	100 , 2',7'-Difluoro-3',6'-bis((4-nitrobenzyl)oxy)-3 <i>H</i> -spiro[isobenzofuran-1,9'-xanthen]-3-one	457–487nm/ 503–538nm	NR	NR	NR
35.	101 , 2',7'-Difluoro-3',6'-bis((5-nitrofurano-2-yl)methoxy)-3 <i>H</i> -spiro[isobenzofuran-1,9'-xanthen]-3-one	457–487nm/503–538nm	1.1 μ M	NR	NR
36.	102 , 2',7'-Difluoro-3',6'-bis((5-nitrothiophen-2-yl)methoxy)-3 <i>H</i> -spiro[isobenzofuran-1,9'-xanthen]-3-one	457–487nm/503–538nm	1 μ M	NR	NR
37.	103 , 2',7'-Difluoro-3',6'-bis((1-methyl-2-nitro-1 <i>H</i> -imidazol-5-yl)methoxy)-3 <i>H</i> -spiro[isobenzofuran-1,9'-xanthen]-3-one	457–487nm/503–538nm	1.6 μ M	NR	NR
38.	104 , 4-(5,5-difluoro-1, 3, 7, 9-tetramethyl- 5 <i>H</i> - 4 λ ,4, 5 λ ,4-dipyrrolo [1,2- <i>c</i> :2',1'- <i>f</i>] [1,3,2]diazaborinin-10-yl)-1-((5-nitrofurano-2-yl)methyl) pyridin-1-ium-2-ide	470/520nm, 10mM PBS buffer (pH 7.4)	36.29 μ M	0.059 μ M/s	9.6 ng/mL
39.	105 , (<i>E</i>)-4-(2-(5,5-difluoro-1,7,9-trimethyl-10-phenyl-5 <i>H</i> -4 λ ,4,5 λ ,4-dipyrrolo[1,2- <i>c</i> :2',1'- <i>f</i>][1,3,2]diazaborinin-3-yl)vinyl)-2-nitrophenol	558/567nm, hexane 579/590nm, toluene 573/585nm, DCM	NR	NR	NR
40.	106 , 4-(2,8-diethyl-5,5-difluoro-1,9-dimethyl-3,7-bis((<i>E</i>)-4-(4-(piperidin-1-yl)butoxy)styryl)-5 <i>H</i> -4 λ ,4,5 λ ,4-dipyrrolo[1,2- <i>c</i> :2',1'- <i>f</i>][1,3,2]diazaborinin-10-yl)phenyl (4-nitrobenzyl) carbonate	659/686nm, water (10% DMSO)	NR	NR	NR
41.	107 ,(<i>E</i>)-4-(3-(3,4-bis(2-(2-(2-methoxyethoxy)ethoxy)ethoxy)styryl)-5,5-difluoro-1,7,9-trimethyl-5 <i>H</i> -4 λ ,4,5 λ ,4-dipyrrolo[1,2- <i>c</i> :2',1'- <i>f</i>][1,3,2]diazaborinin-10-yl)phenyl(4-nitrobenzyl) carbonate	597/617nm, 10mM PBS buffer (pH7.4, 1% DMSO)	0.57 μ M	0.011 μ M/s	0.9 ng/mL
42.	108 , (<i>E</i>)-(2-(2-cyano-3-(6-ethyl-4, 4-difluoro-5, 7-dimethyl-3-((4-nitrobenzyl)thio)-8-phenyl-3a,4-dihydro-4 λ ,4-dicyclopentaborinin-2-yl)acrylamido)ethyl)triphenyl phosphonium	615/715nm, 50mMTris- HCl buffer (pH7.4, 1% DMSO)	33.70 μ M	46.21 μ M/min	16.8 ng/mL
43.	109 , <i>N</i> ² -(4-((2-amino-4-oxo-3,4-dihydropteridin-7-yl)methyl)amino)benzoyl)- <i>N</i> ⁵ -(2-(2-(4-(5, 5-difluoro-	685/730nm, 10mM PBS buffer	NR	NR	1.52 ng/mL

	7-(4-((4-nitrobenzyl)oxy)phenyl)-1,9-diphenyl-5H-5λ ⁴ ,6λ ⁴ -dipyrrolo[1, 2-c: 2', 1'-f][1, 3, 2]diazaborinin-3-yl)phenoxy) acetamido ethyl)glutamine	(pH7.4)			
44.	114 , 8-nitro-4-propyl-6-((1-(3-(1-(((1R,2R,4R)-2,3,4-trihydroxy-5-(((3S,4R)-2,3,4-trihydroxy-5-(hydroxymethyl)cyclohexyl)oxy)cyclohexyl)methyl)-1H-1,2,3-triazol-4-yl)propanoyl)piperidin-4-yl)oxy)-2H-furo[2,3-h]chromen-2-one	370/455nm water	NR	NR	NR
45.	115 , 2,2',2''-(10-(2-((4-nitrobenzyl)oxy)-2-oxoethyl)-1,4,7,10-tetraazacyclododecane-1,4,7-triyl)triacetic acid, gadolinium(III) complex	NR	NR	NR	24 ng/mL
46.	116 , ruthenium(II) bis(4,7-diphenyl-1,10-phenanthroline (4-(3-(2-nitro-1H-imidazol-1-yl)propyl)-2,2'-bipyridine	463/621nm, Tris buffer (pH 7.4)	NR	NR	NR
47.	117 , 2,2',2''-(10-(2-((4-(3-ethoxy-2-(ethoxy carbonyl)-3-oxoprop-1-en-1-yl)-3-(((4-nitrobenzyl) oxy) carbonyl) amino)phenyl)amino)-2-oxoethyl)-1,4,7,10-tetraazacyclododecane-1,4,7-triyl)triacetic acid)terbium(III) complex	350/550nm, 50mM Tris buffer (pH 7.4)	18.4 μM	0.027 μM/min	4.4 ng/mL
48.	118 , 2,2',2''-(10-(2-(4-amino-1,3-dioxoisindolin-2-yl)ethyl)-1,4,7,10-tetraazacyclododecane-1,4,7-triyl)triacetic acid europium(III) complex	405/525nm, PBS buffer (pH 7.4)	NR	NR	1.78 ng/mL

*NR= Not Reported

6. Notes and References

- Ruddaraju, R. R.; Murugulla, A. C.; Kotla, R.; Tirumalasetty, M. C. B.; Wudayagiri, R.; Donthabakthuni, S.; Maraju, R. Design, Synthesis, Anticancer Activity and Docking Studies of Theophylline Containing 1,2,3-Triazoles with Variant Amide Derivatives. *Medchemcomm* **2017**, *8* (1), 176–183. <https://doi.org/10.1039/c6md00479b>.
- Khamenehfar, A. Reversal of Multidrug Resistance Fluorescently Measured in Single Cancer Cells Captured in the Microfluidic Chip by Avid Khamenehfar Summer 2015. *Reversal Multidrug Resist. Fluoresc. Meas. Single Cancer Cells Captured Microfluid. Chip* **2015**, 1–211.
- Cairns, J. Mutation Selection and the Natural History of Cancer. *Nature* **1975**, *255* (5505), 197–200. <https://doi.org/10.1038/255197a0>.
- Cell Division, Cancer | Learn Science at Scitable <https://www.nature.com/scitable/topicpage/cell-division-and-cancer-14046590/>.
- Shinohara, E.; Maity, A. Increasing Sensitivity to Radiotherapy and Chemotherapy by Using Novel Biological Agents That Alter the Tumor Microenvironment. *Curr. Mol. Med.* **2009**, *9* (9), 1034–1045. <https://doi.org/10.2174/156652409789839107>.
- Brown, J. M.; Wilson, W. R. Exploiting Tumour Hypoxia in Cancer Treatment. *Nature Reviews Cancer*. Nature Publishing Group 2004, pp 437–447. <https://doi.org/10.1038/nrc1367>.
- Yotnda, P.; Wu, D.; Swanson, A. M. Hypoxic Tumors and Their Effect on Immune Cells and Cancer Therapy. *Methods in molecular biology (Clifton, N.J.)*. Humana Press, Totowa, NJ 2010, pp 1–29. https://doi.org/10.1007/978-1-60761-786-0_1.
- Williams, K. J.; Albertella, M. R.; Fitzpatrick, B.; Loadman, P. M.; Shnyder, S. D.; Chinje, E. C.; Telfer, B. A.; Dunk, C. R.; Harris, P. A.; Stratford, I. J. In Vivo Activation of the Hypoxia-Targeted Cytotoxin AQ4N in Human Tumor Xenografts. *Mol. Cancer Ther.* **2009**, *8* (12), 3266–3275. <https://doi.org/10.1158/1535-7163.MCT-09-0396>.
- Muz, B.; de la Puente, P.; Azab, F.; Azab, A. K. The Role of Hypoxia in Cancer Progression, Angiogenesis, Metastasis, and Resistance to Therapy. *Hypoxia* **2015**, *3*, 83–92. <https://doi.org/10.2147/hp.s93413>.
- Kizaka-Kondoh, S.; Inoue, M.; Harada, H.; Hiraoka, M. Tumor Hypoxia: A Target for Selective Cancer Therapy. *Cancer Science*. John Wiley & Sons, Ltd December 1, 2003, pp 1021–1028. <https://doi.org/10.1111/j.1349-7006.2003.tb01395.x>.
- Harris, A. L. Hypoxia - A Key Regulatory Factor in Tumour Growth. *Nature Reviews Cancer*. European Association for Cardio-Thoracic Surgery 2002, pp 38–47. <https://doi.org/10.1038/nrc704>.
- Hickman, J. A.; Potten, C. S.; Merritt, A. J.; Fisher, T. C. Apoptosis and Cancer Chemotherapy. *Philos. Trans. R. Soc. London. Ser. B Biol. Sci.* **1994**, *345* (1313), 319–325. <https://doi.org/10.1098/rstb.1994.0112>.
- Exploiting the Tumor Microenvironment – Threshold, Bioatla, Pfizer | Cancer Biology <https://blogs.shu.edu/cancer/2015/12/16/exploiting-the-tumor-microenvironment-threshold-bioatla-pfizer/>.
- Xie, D.; Kim, S.; Kohli, V.; Banerjee, A.; Yu, M.; Enriquez, J. S.; Luci, J. J.; Que, E. L. Hypoxia-Responsive¹⁹F MRI Probes with Improved Redox Properties and Biocompatibility. *Inorg. Chem.* **2017**, *56* (11), 6429–6437. <https://doi.org/10.1021/acs.inorgchem.7b00500>.
- Huetting, R.; Kersemans, V.; Tredwell, M.; Cornelissen, B.; Christlieb, M.; Gee, A. D.; Passchier, J.; Smart, S. C.; Gouverneur, V.; Muschel, R. J.; et al. A Dual Radiolabelling Approach for Tracking Metal Complexes: Investigating the Speciation of Copper Bis(Thiosemicarbazones) in Vitro and in Vivo. *Metallomics* **2015**, *7* (5), 795–804.

- <https://doi.org/10.1039/c4mt00330f>.
16. Desoize, B. Metals and Metal Compounds in Cancer Treatment. *Anticancer Res.* **2004**, *24* (3 A), 1529–1544.
 17. Ellahioui, Y.; Prashar, S.; Gómez-Ruiz, S. Anticancer Applications and Recent Investigations of Metallo drugs Based on Gallium, Tin and Titanium. *Inorganics* **2017**, *5* (1), 1–23. <https://doi.org/10.3390/inorganics5010004>.
 18. Farrell, N. Metal Complexes as Drugs and Chemotherapeutic Agents. *Met. Complexes as Drugs Chemother. Agents* **2003**, *9*, 809–840.
 19. Dilruba, S.; Kalayda, G. V. Platinum-Based Drugs: Past, Present and Future. *Cancer Chemotherapy and Pharmacology*. Springer Verlag June 1, 2016, pp 1103–1124. <https://doi.org/10.1007/s00280-016-2976-z>.
 20. Lebwohl, D.; Canetta, R. Clinical Development of Platinum Complexes in Cancer Therapy: An Historical Perspective and an Update. *European Journal of Cancer*. September 1998, pp 1522–1534. [https://doi.org/10.1016/S0959-8049\(98\)00224-X](https://doi.org/10.1016/S0959-8049(98)00224-X).
 21. Galanski, M. Recent Developments in the Field of Anticancer Platinum Complexes. *Recent Pat. Anticancer. Drug Discov.* **2008**, *1* (2), 285–295. <https://doi.org/10.2174/15748920677442287>.
 22. Klein, A. V.; Hambley, T. W. Platinum Drug Distribution in Cancer Cells and Tumors. *Chem. Rev.* **2009**, *109* (10), 4911–4920. <https://doi.org/10.1021/cr9001066>.
 23. Jung, Y.; Lippard, S. J. Direct Cellular Responses to Platinum-Induced DNA Damage. *Chemical Reviews*. American Chemical Society May 2007, pp 1387–1407. <https://doi.org/10.1021/cr068207j>.
 24. Jia, P.; Ouyang, R.; Cao, P.; Tong, X.; Zhou, X.; Lei, T.; Zhao, Y.; Guo, N.; Chang, H.; Miao, Y.; et al. Review: Recent Advances and Future Development of Metal Complexes as Anticancer Agents. *J. Coord. Chem.* **2017**, *70* (13), 2175–2201. <https://doi.org/10.1080/00958972.2017.1349313>.
 25. Shaili, E. Platinum Anticancer Drugs and Photochemotherapeutic Agents: Recent Advances and Future Developments. *Sci. Prog.* **2014**, *97* (1), 20–40. <https://doi.org/10.3184/003685014x13904811808460>.
 26. Johnstone, T. C.; Suntharalingam, K.; Lippard, S. J. *Third Row Transition Metals for the Treatment of Cancer*, 2015; Vol. 373. <https://doi.org/10.1098/rsta.2014.0185>.
 27. Trudu, F.; Amato, F.; Vaňhara, P.; Pivetta, T.; Peñá-Méndez, E. M.; Havel, J. Coordination Compounds in Cancer: Past, Present and Perspectives. *J. Appl. Biomed.* **2015**, *13* (2), 79–103. <https://doi.org/10.1016/j.jab.2015.03.003>.
 28. Ozols, R. F.; Bundy, B. N.; Greer, B. E.; Fowler, J. M.; Clarke-Pearson, D.; Burger, R. A.; Mannel, R. S.; DeGeest, K.; Hartenbach, E. M.; Baergen, R.; et al. Phase III Trial of Carboplatin and Paclitaxel Compared with Cisplatin and Paclitaxel in Patients with Optimally Resected Stage III Ovarian Cancer: A Gynecologic Oncology Group Study. *J. Clin. Oncol.* **2003**, *21* (17), 3194–3200. <https://doi.org/10.1200/JCO.2003.02.153>.
 29. Wheate, N. J.; Walker, S.; Craig, G. E.; Oun, R. The Status of Platinum Anticancer Drugs in the Clinic and in Clinical Trials. *Dalton. Trans.* **2010**, *39* (35), 8113–8127. <https://doi.org/10.1039/c0dt00292e>.
 30. Comella, P.; Casaretti, R.; Sandomenico, C.; Avallone, A.; Franco, L. Role of Oxaliplatin in the Treatment of Colorectal Cancer. *Therapeutics and Clinical Risk Management*. Dove Medical Press Ltd. 2009, pp 229–238. <https://doi.org/10.2147/tcrm.s3583>.
 31. Hang, Z.; Cooper, M. A.; Ziora, Z. M. Platinum-Based Anticancer Drugs Encapsulated Liposome and Polymeric Micelle Formulation in Clinical Trials. *Biochem. Compd.* **2016**, *4* (1), 1. <https://doi.org/10.7243/2052-9341-4-2>.
 32. Gietema, J. A.; Veldhuis, G. J.; Guchelaar, H. J.; Willemsse, P. H. B.; Uges, D. R. A.; Cats, A.; Boonstra, H.; van der Graaf, W. T. A.; Sleijfer, D. T.; de Vries, E. G. E.; et al. Phase II and Pharmacokinetic Study of Lobaplatin in Patients with Relapsed Ovarian Cancer. *Br. J. Cancer* **1995**, *71* (6), 1302–1307. <https://doi.org/10.1038/bjc.1995.252>.
 33. Welink, J.; Boven, E.; Vermorken, J. B.; Gall, H. E.; van der Vijgh, W. J. F. Pharmacokinetics and Pharmacodynamics of Lobaplatin (D-19466) in Patients with Advanced Solid Tumors, Including Patients with Impaired Renal or Liver Function. *Clin. Cancer Res.* **1999**, *5* (9), 2349–2358.
 34. (34) Wang, X.; Guo, Z. The Role of Sulfur in Platinum Anticancer Chemotherapy. *Anticancer. Agents Med. Chem.* **2008**, *7* (1), 19–34. <https://doi.org/10.2174/187152007779314062>.
 35. Gietema, J. A.; De Vries, E. G. E.; Sleijfer, D. T.; Willemsse, P. H. B.; Guchelaar, H. J.; Uges, D. R. A.; Aulenbacher, P.; Voegeli, R.; Mulder, N. H. A Phase I Study of 1, 2-Diamminomethyl-Cyclobutane-Platinum (II)-Lactate (D-19466; Lobaplatin) Administered Daily for 5 Days. *Br. J. Cancer* **1993**, *67* (2), 396–401. <https://doi.org/10.1038/bjc.1993.73>.
 36. Mross, K.; Meyberg, F.; Fiebig, H. H.; Hamm, K.; Hieber, U.; Aulenbacher, P.; Hossfeld, D. K. Pharmacokinetic and Pharmacodynamic Study with Lobaplatin (D-19466), a New Platinum Complex, after Bolus Administration. *Oncol. Res. Treat.* **1992**, *15* (2), 139–146. <https://doi.org/10.1159/000217347>.
 37. *Lobaplatin D 19466*; 2003; Vol. 4. <https://doi.org/10.2165/00126839-200304060-00008>.
 38. Choi, C. H.; Cha, Y. J.; An, C. S.; Kim, K. J.; Kim, K. C.; Moon, S. P.; Lee, Z. H.; Min, Y. D. Molecular Mechanisms of Heptaplatin Effective against Cisplatin-Resistant Cancer Cell Lines: Less Involvement of Metallothionein. *Cancer Cell Int.* **2004**, *4* (1), 1–12. <https://doi.org/10.1186/1475-2867-4-6>.
 39. Lee, J. W.; Park, J. K.; Lee, S. H.; Kim, S. Y.; Cho, Y. B.; Kuh, H. J. Anti-Tumor Activity of Heptaplatin in Combination with 5-Fluorouracil or Paclitaxel against Human Head and Neck Cancer Cells in Vitro. *Anticancer. Drugs* **2006**, *17* (4), 377–384. <https://doi.org/10.1097/01.cad.0000205033.08838.c7>.
 40. Jeenvanram, R.; Shah, D.; Kumar, B.; Sharma, S.; Ganatra, R. Synthesis of Thyroglobulin in Thyroid Carcinoma Patients after Radioiodine Therapy. *Cancer* **1983**, *52* (12), 2240–2244. <https://doi.org/10.1002/1097-0142>.
 41. Lee, K. H.; Hyun, M. S.; Kim, H.-K.; Jin, H. M.; Yang, J.; Song, H. S.; Do, Y. R.; Ryoo, H. M.; Chung, J. S.; Zang, D. Y.; et al. Randomized, Multicenter, Phase III

- Trial of Heptaplatin 1-Hour Infusion and 5-Fluorouracil Combination Chemotherapy Comparing with Cisplatin and 5-Fluorouracil Combination Chemotherapy in Patients with Advanced Gastric Cancer. *Cancer Res. Treat.* **2009**, *41* (1), 12–18. <https://doi.org/10.4143/crt.2009.41.1.12>.
42. Battle, A. R.; Choi, R.; Hibbs, D. E.; Hambley, T. W. Platinum(IV) Analogues of AMD473 (Cis-[PtCl₂(NH₃)(2-Picoline)]: Preparative, Structural, and Electrochemical Studies. *Inorg. Chem.* **2006**, *45* (16), 6317–6322. <https://doi.org/10.1021/ic060273g>.
 43. Holford, J.; Raynaud, F.; Murrer, B. A.; Grimaldi, K.; Hartley, J. A.; Abrams, M.; Kelland, L. R. Chemical, Biochemical and Pharmacological Activity of the Novel Sterically Hindered Platinum Co-Ordination Complex, Cis-[Amminedichloro(2-Methylpyridine)] Platinum(II) (AMD473). *Anticancer. Drug Des.* **1998**, *13* (1), 1–18.
 44. Sharp, S. Y.; O'Neill, C. F.; Rogers, P.; Boxall, F. E.; Kelland, L. R. Retention of Activity by the New Generation Platinum Agent AMD0473 in Four Human Tumour Cell Lines Possessing Acquired Resistance to Oxaliplatin. *Eur. J. Cancer* **2002**, *38* (17), 2309–2315. [https://doi.org/10.1016/S0959-8049\(02\)00244-7](https://doi.org/10.1016/S0959-8049(02)00244-7).
 45. Beale, P.; Judson, I.; O'Donnell, A.; Trigo, J.; Rees, C.; Raynaud, F.; Turner, A.; Simmons, L.; Etterley, L. A Phase I Clinical and Pharmacological Study of Cis-Diamminedichloro(2-Methylpyridine) Platinum II (AMD473). *Br. J. Cancer* **2003**, *88* (7), 1128–1134. <https://doi.org/10.1038/sj.bjc.6600854>.
 46. Eckardt, J. R.; Bentsion, D. L.; Lipatov, O. N.; Polyakov, I. S.; MacKintosh, F. R.; Karlin, D. A.; Baker, G. S.; Breit, H. B. Phase II Study of Picoplatin as Second-Line Therapy for Patients with Small-Cell Lung Cancer. *J. Clin. Oncol.* **2009**, *27* (12), 2046–2051. <https://doi.org/10.1200/JCO.2008.19.3235>.
 47. Wheate, N. J.; Walker, S.; Craig, G. E.; Oun, R. The Status of Platinum Anticancer Drugs in the Clinic and in Clinical Trials. *Dalton. Trans.* **2010**, *39* (35), 8113–8127. <https://doi.org/10.1039/c0dt00292e>.
 48. Hall, M. D.; Mellor, H. R.; Callaghan, R.; Hambley, T. W. Basis for Design and Development of Platinum(IV) Anticancer Complexes. *J. Med. Chem.* **2007**, *50* (15), 3403–3411. <https://doi.org/10.1021/jm070280u>.
 49. Samimi, G.; Howell, S. B. Modulation of the Cellular Pharmacology of JM118, the Major Metabolite of Satraplatin, by Copper Influx and Efflux Transporters. *Cancer Chemother. Pharmacol.* **2006**, *57* (6), 781–788. <https://doi.org/10.1007/s00280-005-0121-5>.
 50. Choy, H.; Park, C.; Yao, M. Current Status and Future Prospects for Satraplatin, an Oral Platinum Analogue. *Clin. Cancer Res.* **2008**, *14* (6), 1633–1638. <https://doi.org/10.1158/1078-0432.CCR-07-2176>.
 51. Cmelak, A. J.; Murphy, B. A.; Day, T. Combined-Modality Therapy for Locoregionally Advanced Head and Neck Cancer. *Oncology* **1999**, *13* (10 SUPPL. 5), 83–91.
 52. Bouchal, P.; Jarkovsky, J.; Hrazdilova, K.; Dvorakova, M.; Struharova, I.; Hernychova, L.; Damborsky, J.; Sova, P.; Vojtesek, B. The New Platinum-Based Anticancer Agent LA-12 Induces Retinol Binding Protein 4 in Vivo. *Proteome Sci.* **2011**, *9* (1), 1–9. <https://doi.org/10.1186/1477-5956-9-68>.
 53. Kvardova, V.; Hrstka, R.; Walerych, D.; Muller, P.; Matoukova, E.; Hruskova, V.; Stelcova, D.; Sova, P.; Vojtesek, B. The New Platinum(IV) Derivative LA-12 Shows Stronger Inhibitory Effect on Hsp90 Function Compared to Cisplatin. *Mol. Cancer* **2010**, *9* (1), 1–9. <https://doi.org/10.1186/1476-4598-9-147>.
 54. Kozubík, A.; Horváth, V.; Šviháková-Šindlerová, L.; Souček, K.; Hofmanová, J.; Sova, P.; Kroutil, A.; Žák, F.; Mistr, A.; Turánek, J. High Effectiveness of Platinum(IV) Complex with Adamantylamine in Overcoming Resistance to Cisplatin and Suppressing Proliferation of Ovarian Cancer Cells in Vitro. *Biochem. Pharmacol.* **2005**, *69* (3), 373–383. <https://doi.org/10.1016/j.bcp.2004.09.005>.
 55. Howell, S. B. The Design and Development of the Tumor-Targeting Nanopolymer DACH Platinum Conjugate AP5346 (Prolindac™). *Platin. Other Heavy Met. Compd. Cancer Chemother.* **2009**, 33–39. https://doi.org/10.1007/978-1-60327-459-3_5.
 56. Nowotnik, D. P.; Cvitkovic, E. ProLindac™ (AP5346): A Review of the Development of an HPMA DACH Platinum Polymer Therapeutic. *Adv. Drug Deliv. Rev.* **2009**, *61* (13), 1214–1219. <https://doi.org/10.1016/j.addr.2009.06.004>.
 57. Sood, P.; Bruce Thurmond, K.; Jacob, J. E.; Waller, L. K.; Silva, G. O.; Stewart, D. R.; Nowotnik, D. P. Synthesis and Characterization of AP5346, a Novel Polymer-Linked Diaminocyclohexyl Platinum Chemotherapeutic Agent. *Bioconjugate. Chem.* **2006**, *17* (5), 1270–1279. <https://doi.org/10.1021/bc0600517>.
 58. Gianasi, E.; Wasil, M.; Evagorou, E. G.; Keddle, A.; Wilson, G.; Duncan, R. HPMA Copolymer Platinates as Novel Antitumour Agents: In Vitro Properties, Pharmacokinetics and Antitumour Activity in Vivo. *Eur. J. Cancer* **1999**, *35* (6), 994–1002. [https://doi.org/10.1016/S0959-8049\(99\)00030-1](https://doi.org/10.1016/S0959-8049(99)00030-1).
 59. Smith, B. R.; Heverhagen, J.; Knopp, M.; Schmalbrock, P.; Shapiro, J.; Shiomi, M.; Moldovan, N. I.; Ferrari, M.; Lee, S. C. Localization to Atherosclerotic Plaque and Biodistribution of Biochemically Derivatized Superparamagnetic Iron Oxide Nanoparticles (SPIONs) Contrast Particles for Magnetic Resonance Imaging (MRI). *Biomed. Microdevices* **2007**, *9* (5), 719–727. <https://doi.org/10.1007/s10544-007-9081-3>.
 60. Campone, M.; Rademaker-Lakhai, J. M.; Bennouna, J.; Howell, S. B.; Nowotnik, D. P.; Beijnen, J. H.; Schellens, J. H. M. Phase I and Pharmacokinetic Trial of AP5346, a DACH-Platinum-Polymer Conjugate, Administered Weekly for Three out of Every 4 Weeks to Advanced Solid Tumor Patients. *Cancer Chemother. Pharmacol.* **2007**, *60*, 523–533. <https://doi.org/10.1007/s00280-006-0397-0>.
 61. Purohit, P.; Kumar, S.; Sharma, V.; Singh, M. Thirty Six Year Old Platinum as an Anticancer Agent. *Indo Glob. J. Pharm. Sci.* **2018**, *08* (01), 26–32. <https://doi.org/10.35652/igjps.2018.2632>.
 62. Browning, R. J.; Reardon, P. J. T.; Parhizkar, M.; Pedley, R. B.; Edirisinghe, M.; Knowles, J. C.; Stride, E. Drug Delivery Strategies for Platinum-Based Chemotherapy. *ACS Nano* **2017**, *11* (9), 8560–8578. <https://doi.org/10.1021/acsnano.7b04092>.
 63. Rashighi, M.; Harris, J. E. The Next Generation of Platinum Drugs: Targeted Pt(II) Agents, Nanoparticle Delivery, and Pt(IV) Prodrugs. *Physiol. Behav.* **2017**, *176* (3), 139–148. <https://doi.org/10.1053/j.gastro.2016.08.014>.
 64. Mjos, K. D.; Orvig, C. Metallodrugs in Medicinal

- Inorganic Chemistry. *Chemical Reviews*. 2014, pp 4540–4563. <https://doi.org/10.1021/cr400460s>.
65. Chen, W.; Ou, W.; Wang, L.; Hao, Y.; Cheng, J.; Li, J.; Liu, Y. N. Synthesis and Biological Evaluation of Hydroxyl-Substituted Schiff-Bases Containing Ferrocenyl Moieties. *Dalton. Trans.* **2013**, 42 (44), 15678–15686. <https://doi.org/10.1039/c3dt51977e>.
 66. Frezza, M.; Hindo, S.; Chen, D.; Davenport, A.; Schmitt, S.; Tomco, D.; Ping Dou, Q. Novel Metals and Metal Complexes as Platforms for Cancer Therapy. *Curr. Pharm. Des.* **2010**, 16 (16), 1813–1825. <https://doi.org/10.2174/138161210791209009>.
 67. Yang, H.; Villani, R. M.; Wang, H.; Simpson, M. J.; Roberts, M. S.; Tang, M.; Liang, X. The Role of Cellular Reactive Oxygen Species in Cancer Chemotherapy. *J. Exp. Clin. Cancer Res.* **2018**, 37 (1), 1–10. <https://doi.org/10.1186/s13046-018-0909-x>.
 68. Jungwirth, U.; Kowol, C. R.; Keppler, B. K.; Hartinger, C. G.; Berger, W.; Heffeter, P. Anticancer Activity of Metal Complexes: Involvement of Redox Processes. *Antioxidants Redox Signal.* **2011**, 15 (4), 1085–1127. <https://doi.org/10.1089/ars.2010.3663>.
 69. Wang, J.; Yi, J. Cancer Cell Killing via ROS: To Increase or Decrease, That Is a Question. *Cancer Biology and Therapy*. Landes Bioscience December 28, 2008, pp 1875–1884. <https://doi.org/10.4161/cbt.7.12.7067>.
 70. Conklin, K. A. Chemotherapy-Associated Oxidative Stress: Impact on Chemotherapeutic Effectiveness. *Integr. Cancer Ther.* **2004**, 3 (4), 294–300. <https://doi.org/10.1177/1534735404270335>.
 71. Zhang, P.; Sadler, P. J. Redox-Active Metal Complexes for Anticancer Therapy. *European Journal of Inorganic Chemistry*. Wiley-VCH Verlag 2017, pp 1541–1548. <https://doi.org/10.1002/ejic.201600908>.
 72. Santini, C.; Pellei, M.; Gandin, V.; Porchia, M.; Tisato, F.; Marzano, C. Advances in Copper Complexes as Anticancer Agents. *Chem. Rev.* **2014**, 114 (1), 815–862. <https://doi.org/10.1021/cr400135x>.
 73. Taylor, A. B.; Stoj, C. S.; Ziegler, L.; Kosman, D. J.; Hart, P. J. The Copper-Iron Connection in Biology: Structure of the Metallo-Oxidase Fet3p. *Proc. Natl. Acad. Sci.* **2005**, 102 (43), 15459–15464. <https://doi.org/10.1073/pnas.0506227102>.
 74. Goldstein, S.; Czapski, G. The Role and Mechanism of Metal Ions and Their Complexes in Enhancing Damage in Biological Systems or in Protecting These Systems from These Systems from the Toxicity of O₂. *J. Free Radicals Biol. Med.* **1986**, 2 (1), 3–11. [https://doi.org/10.1016/0748-5514\(86\)90117-0](https://doi.org/10.1016/0748-5514(86)90117-0).
 75. Filomeni, G.; Cerchiaro, G.; Da Costa Ferreira, A. M.; De Martino, A.; Pedersen, J. Z.; Rotilio, G.; Ciriolo, M. R. Pro-Apoptotic Activity of Novel Isatin-Schiff Base Copper(II) Complexes Depends on Oxidative Stress Induction and Organelle-Selective Damage. *J. Biol. Chem.* **2007**, 282 (16), 12010–12021. <https://doi.org/10.1074/jbc.M610927200>.
 76. Ott, I.; Gust, R. Non Platinum Metal Complexes as Anti-Cancer Drugs. *Arch. Pharm. (Weinheim)*. **2007**, 340 (3), 117–126. <https://doi.org/10.1002/ardp.200600151>.
 77. Desoize, B. Metals and Metal Compounds in Cancer Treatment. *Anticancer Res.* **2004**, 1544 (24), 1529–1544.
 78. Caruso, F.; Rossi, M. Antitumor Titanium Compounds. *Mini-Reviews Med. Chem.* **2005**, 4 (1), 49–60. <https://doi.org/10.2174/1389557043487565>.
 79. Harding, M.; Mokdsi, G. Antitumor Metalloenes: Structure-Activity Studies and Interactions with Biomolecules. *Curr. Med. Chem.* **2012**, 7 (12), 1289–1303. <https://doi.org/10.2174/0929867003374066>.
 80. Köpf-Maier, P. Complexes of Metals Other than Platinum as Antitumor Agents. *Eur. J. Clin. Pharmacol.* **1994**, 47 (1), 1–16. <https://doi.org/10.1007/BF00193472>.
 81. Meléndez, E. Titanium Complexes in Cancer Treatment. *Critical Reviews in Oncology/Hematology*. Elsevier June 1, 2002, pp 309–315. [https://doi.org/10.1016/S1040-8428\(01\)00224-4](https://doi.org/10.1016/S1040-8428(01)00224-4).
 82. Keppler, B. K.; Hartmann, M. New Tumor-Inhibiting Metal Complexes. Chemistry and Antitumor Properties. *Met. Based. Drugs* **1994**, 1 (2–3), 145–149. <https://doi.org/10.1155/mbd.1994.145>.
 83. (83) Caruso, F.; Rossi, M.; Opazo, C.; Pettinari, C. Structural Features of Antitumor Titanium Agents and Related Compounds. *Bioinorg. Chem. Appl.* **2005**, 2005 (3–4), 317–329. <https://doi.org/10.1155/BCA.2005.317>.
 84. Prihantono; Irfandi, R.; Raya, I.; Warsinggih. Potential Anticancer Activity of Mn (II) Complexes Containing Arginine Dithiocarbamate Ligand on MCF-7 Breast Cancer Cell Lines. *Ann. Med. Surg.* **2020**, 60, 396–402. <https://doi.org/10.1016/j.amsu.2020.11.018>.
 85. Batinic-Haberle, I.; Tovmasyan, A.; Spasojevic, I. Mn Porphyrin-Based Redox-Active Drugs: Differential Effects as Cancer Therapeutics and Protectors of Normal Tissue against Oxidative Injury. *Antioxidants Redox Signal.* **2018**, 29 (16), 1691–1724. <https://doi.org/10.1089/ars.2017.7453>.
 86. Heer, C. D.; Davis, A. B.; Riffe, D. B.; Wagner, B. A.; Falls, K. C.; Allen, B. G.; Buettner, G. R.; Beardsley, R. A.; Riley, D. P.; Spitz, D. R. Superoxide Dismutase Mimetic GC4419 Enhances the Oxidation of Pharmacological Ascorbate and Its Anticancer Effects in an H₂O₂-Dependent Manner. *Antioxidants* **2018**, 7 (1), 1–13. <https://doi.org/10.3390/antiox7010018>.
 87. Borgstahl, G. E. O.; Oberley-Deegan, R. E. Superoxide Dismutases (SODs) and SOD Mimetics. *Antioxidants* **2018**, 7 (11), 1–3. <https://doi.org/10.3390/antiox7110156>.
 88. Torti, S. V.; Torti, F. M. Iron and Cancer: More Ore to Be Mined. *Nat. Rev. Cancer* **2013**, 13 (5), 342–355. <https://doi.org/10.1038/nrc3495>.
 89. Wani, W. A.; Baig, U.; Shreaz, S.; Shiekh, R. A.; Iqbal, P. F.; Jameel, E.; Ahmad, A.; Mohd-Setapar, S. H.; Mushtaque, M.; Ting Hun, L. Recent Advances in Iron Complexes as Potential Anticancer Agents. *New J. Chem.* **2016**, 40 (2), 1063–1090. <https://doi.org/10.1039/c5nj01449b>.
 90. Vessieres, A. Iron Compounds as Anticancer Agents. *RSC Met.* **2019**, 2019 (14), 62–90. <https://doi.org/10.1039/9781788016452-00062>.
 91. Wong, E. L. M.; Fang, G. S.; Che, C. M.; Zhu, N. Highly Cytotoxic Iron(II) Complexes with Pentadentate Pyridyl Ligands as a New Class of Anti-Tumor Agents. *Chem. Commun.* **2005**, No. 36, 4578–4580. <https://doi.org/10.1039/b507687k>.
 92. Kwong, W. L.; Lok, C. N.; Tse, C. W.; Wong, E. L. M.; Che, C. M. Anti-Cancer Iron(II) Complexes of Pentadentate N-Donor Ligands: Cytotoxicity,

- Transcriptomics Analyses, and Mechanisms of Action. *Chem. Eur. J.* **2015**, *21* (7), 3062–3072. <https://doi.org/10.1002/chem.201404749>.
93. Hille, A.; Ott, I.; Kitanovic, A.; Kitanovic, I.; Alborzina, H.; Lederer, E.; Wölfl, S.; Metzler-Nolte, N.; Schäfer, S.; Sheldrick, W. S.; et al. [N,N'-Bis(Salicylidene)-1,2-Phenylenediamine]Metal Complexes with Cell Death Promoting Properties. *J. Biol. Inorg. Chem.* **2009**, *14* (5), 711–725. <https://doi.org/10.1007/s00775-009-0485-9>.
94. Lange, T. S.; Kim, K. K.; Singh, R. K.; Strongin, R. M.; McCourt, C. K.; Brard, L. Iron(III)-Salophene: An Organometallic Compound with Selective Cytotoxic and Anti-Proliferative Properties in Platinum-Resistant Ovarian Cancer Cells. *PLoS One* **2008**, *3* (5), 1–10.
95. Kim, K. K.; Singh, R. K.; Strongin, R. M.; Moore, R. G.; Brard, L.; Lange, T. S. Organometallic Iron(III)-Salophene Exerts Cytotoxic Properties in Neuroblastoma Cells via Mapk Activation and Ros Generation. *PLoS One* **2011**, *6* (4), 19049–19059. <https://doi.org/10.1371/journal.pone.0019049>.
96. Basu, U.; Khan, I.; Hussain, A.; Kondaiah, P.; Chakravarty, A. R. Photodynamic Effect in Near-IR Light by a Photocytotoxic Iron(III) Cellular Imaging Agent. *Angew. Chem. Int. Ed.* **2012**, *51* (11), 2658–2661. <https://doi.org/10.1002/anie.201108360>.
97. Basu, U.; Pant, I.; Khan, I.; Hussain, A.; Kondaiah, P.; Chakravarty, A. R. Iron(III) Catecholates for Cellular Imaging and Photocytotoxicity in Red Light. *Chem. Asian J.* **2014**, *9* (9), 2494–2504. <https://doi.org/10.1002/asia.201402207>.
98. Basu, U.; Pant, I.; Kondaiah, P.; Chakravarty, A. R. Mitochondria-Targeting Iron(III) Catecholates for Photoactivated Anticancer Activity under Red Light. *Eur. J. Inorg. Chem.* **2016**, *2016* (7), 1002–1012. <https://doi.org/10.1002/ejic.201501105>.
99. Sigel, A.; Sigel, H.; Sigel, R. K. O. Interrelations between Essential Metal Ions and Human Diseases. *Met. Ions Life Sci.* **2013**, *13*, 1–535.
100. Munteanu, C. R.; Suntharalingam, K. Advances in Cobalt Complexes as Anticancer Agents. *Dalton. Trans.* **2015**, *44* (31), 13796–13808. <https://doi.org/10.1039/c5dt02101d>.
101. Ware, D. C.; Palmer, B. D.; Wilson, W. R.; Denny, W. A. Hypoxia-Selective Antitumor Agents. 7. Metal Complexes of Aliphatic Mustards as a New Class of Hypoxia-Selective Cytotoxins. Synthesis and Evaluation of Cobalt(III) Complexes of Bidentate Mustards. *J. Med. Chem.* **1993**, *36* (13), 1839–1846. <https://doi.org/10.1021/jm00065a006>.
102. Ahn, G. O.; Ware, D. C.; Denny, W. A.; Wilson, W. R. Optimization of the Auxiliary Ligand Shell of Cobalt(III)(8-Hydroxyquinoline) Complexes as Model Hypoxia-Selective Radiation-Activated Prodrugs. *Radiat. Res.* **2004**, *162* (3), 315–325. <https://doi.org/10.1667/RR3229>.
103. Gust, R.; Ott, I.; Posselt, D.; Sommer, K. Development of Cobalt(3,4-Diarylsalen) Complexes as Tumor Therapeutics. *J. Med. Chem.* **2004**, *47* (24), 5837–5846. <https://doi.org/10.1021/jm040763n>.
104. Failes, T. W.; Cullinane, C.; Diakos, C. I.; Yamamoto, N.; Lyons, J. G.; Hambley, T. W. Studies of a Cobalt(III) Complex of the MMP Inhibitor Marimastat: A Potential Hypoxia-Activated Prodrug. *Chem. Eur. J.* **2007**, *13* (10), 2974–2982. <https://doi.org/10.1002/chem.200601137>.
105. Ivina Paula de Souza. Copper Complexes-A Alternative to Metalloodrugs in Chemotherapy. *Drug Des. Intellect. Prop. Int. J.* **2019**, *3* (2), 1–10.
106. Khan, M. H.; Cai, M.; Deng, J.; Yu, P.; Liang, H.; Yang, F. Anticancer Function and ROS-Mediated Multi-Targeting Anticancer Mechanisms of Copper (II) 2-Hydroxy-1-Naphthaldehyde Complexes. *Molecules* **2019**, *24* (14), 3–20. <https://doi.org/10.3390/molecules24142544>.
107. Hedley, D.; Shamas-Din, A.; Chow, S.; Sanfelice, D.; Schuh, A. C.; Brandwein, J. M.; Seftel, M. D.; Gupta, V.; Yee, K. W. L.; Schimmer, A. D. A Phase I Study of Elesclomol Sodium in Patients with Acute Myeloid Leukemia. *Leuk. Lymphoma* **2016**, *57* (10), 2437–2440. <https://doi.org/10.3109/10428194.2016.1138293>.
108. Monk, B. J.; Kauderer, J. T.; Moxley, K. M.; Bonebrake, A. J.; Dewdney, S. B.; Secord, A. A.; Ueland, F. R.; Johnston, C. M.; Aghajanian, C. A Phase II Evaluation of Elesclomol Sodium and Weekly Paclitaxel in the Treatment of Recurrent or Persistent Platinum-Resistant Ovarian, Fallopian Tube or Primary Peritoneal Cancer: An NRG Oncology/Gynecologic Oncology Group Study. *Gynecol. Oncol.* **2018**, *151* (3), 422–427. <https://doi.org/10.1016/j.ygyno.2018.10.001>.
109. Kirshner, J. R.; He, S.; Balasubramanyam, V.; Kepros, J.; Yang, C. Y.; Zhang, M.; Du, Z.; Barsoum, J.; Bertin, J. Elesclomol Induces Cancer Cell Apoptosis through Oxidative Stress. *Mol. Cancer Ther.* **2008**, *7* (8), 2319–2327. <https://doi.org/10.1158/1535-7163.MCT-08-0298>.
110. Ruiz-Azuara, L.; Bastian, G.; Bravo-Gómez, M. E.; Cañas, R. C.; Flores-Alamo, M.; Fuentes, I.; Mejía, C.; García-Ramos, J. C.; Serrano, A. Abstract CT408: Phase I Study of One Mixed Chelates Copper(II) Compound, Casiopeína CasIIIa with Antitumor Activity and Its Mechanism of Action. In *Cancer Research*; 2014; Vol. 74, pp 1538–7445. <https://doi.org/10.1158/1538-7445.am2014-ct408>.
111. Espinal-Enríquez, J.; Hernández-Lemus, E.; Mejía, C.; Ruiz-Azuara, L. Network Analysis Shows Novel Molecular Mechanisms of Action for Copper-Based Chemotherapy. *Front. Physiol.* **2016**, *6* (JAN), 1–13. <https://doi.org/10.3389/fphys.2015.00406>.
112. Collery, P.; Keppler, B.; Madoulet, C.; Desoize, B. Gallium in Cancer Treatment. *Crit. Rev. Oncol. Hematol.* **2002**, *42* (3), 283–296. [https://doi.org/10.1016/S1040-8428\(01\)00225-6](https://doi.org/10.1016/S1040-8428(01)00225-6).
113. Hart, M. M.; Adamson, R. H. Antitumor Activity and Toxicity of Salts of Inorganic Group 3a Metals: Aluminum, Gallium, Indium, and Thallium. *Proc. Natl. Acad. Sci. U. S. A.* **1971**, *68* (7), 1623–1626. <https://doi.org/10.1073/pnas.68.7.1623>.
114. Hart, M. M.; Smith, C. F.; Yancey, S. T.; Adamson, R. H. Toxicity and Antitumor Activity of Gallium Nitrate and Periodically Related Metal Salts. *J. Natl. Cancer Inst.* **1971**, *47* (5), 1121–1127. <https://doi.org/10.1093/jnci/47.5.1121>.
115. C. R. Chitambar. Gallium-Containing Anticancer Compounds. *Future Med. Chem.* **2012**, *4* (10), 1257–1272.
116. Chitambar, C. R. Gallium Complexes as Anticancer Drugs. *Met. Ions Life Sci.* **2018**, *18*, 281–301. <https://doi.org/10.1515/9783110470734-016>.
117. Yeo, C. I.; Ooi, K. K.; Tiekink, E. R. T. Gold-Based

- Medicine: A Paradigm Shift in Anti-Cancer Therapy? *Molecules* **2018**, *23* (6), 1–26. <https://doi.org/10.3390/molecules23061410>.
118. B. G. Singh, K.; P. Grant, M.; W. Harper, B.; M. Krause-Heuer, A.; Manohar, M.; Orkey, N.; R. Aldrich-Wright, J. Transition Metal Based Anticancer Drugs. *Curr. Top. Med. Chem.* **2011**, *11* (5), 521–542. <https://doi.org/10.2174/156802611794785226>.
119. Fernández-Moreira, V.; Herrera, R. P.; Gimeno, M. C. Anticancer Properties of Gold Complexes with Biologically Relevant Ligands. *Pure Appl. Chem.* **2019**, *91* (2), 247–269. <https://doi.org/10.1515/pac-2018-0901>.
120. Raza, A.; Rasheed, T.; Nabeel, F.; Hayat, U.; Bilal, M.; Iqbal, H. M. N. Endogenous and Exogenous Stimuli-Responsive Drug Delivery Systems for Programmed Site-Specific Release. *Molecules* **2019**, *24* (6), 1–21. <https://doi.org/10.3390/molecules24061117>.
121. Morales-Cruz, M.; Delgado, Y.; Castillo, B.; Figueroa, C. M.; Molina, A. M.; Torres, A.; Milián, M.; Griebenow, K. Smart Targeting to Improve Cancer Therapeutics. *Drug Des. Devel. Ther.* **2019**, *13*, 3753–3772. <https://doi.org/10.2147/DDDT.S219489>.
122. Zhou, J.; Shi, W.; Li, L. H.; Gong, Q. Y.; Wu, X. F.; Li, X. H.; Ma, H. M. A Lysosome-Targeting Fluorescence Off-On Probe for Imaging of Nitroreductase and Hypoxia in Live Cells. *Chem. Asian J.* **2016**, *11* (19), 2719–2724. <https://doi.org/10.1002/asia.201600012>.
123. Liu, Z. R.; Tang, Y.; Xu, A.; Lin, W. A New Fluorescent Probe with a Large Turn-on Signal for Imaging Nitroreductase in Tumor Cells and Tissues by Two-Photon Microscopy. *Biosens. Bioelectron.* **2017**, *89* (July 2016), 853–858. <https://doi.org/10.1016/j.bios.2016.09.107>.
124. Ciesienki, K. L.; Franz, K. J. Keys for Unlocking Photolabile Metal-Containing Cages. *Angew. Chem. Int. Ed.* **2011**, *50* (4), 814–824. <https://doi.org/10.1002/anie.201002542>.
125. Kim, H. M.; Cho, B. R. Small-Molecule Two-Photon Probes for Bioimaging Applications. *Chem. Rev.* **2015**, *115* (11), 5014–5055. <https://doi.org/10.1021/cr5004425>.
126. Qiao, J.; Wang, M.; Cui, M.; Fang, Y.; Li, H.; Zheng, C.; Li, Z.; Xu, Y.; Hua, H.; Li, D. Small-Molecule Probes for Fluorescent Detection of Cellular Hypoxia-Related Nitroreductase. *J. Pharm. Biomed. Anal.* **2021**, *203*, 114199. <https://doi.org/10.1016/j.jpba.2021.114199>.
127. Brieke, C.; Rohrbach, F.; Gottschalk, A.; Mayer, G.; Heckel, A. Light-Controlled Tools. *Angew. Chem. Rev.* **2012**, *51*, 2–33. <https://doi.org/10.1002/anie.201202134>.
128. Lu, C. C.; Bill, E.; Weyhermüller, T.; Bothe, E.; Wieghardt, K. Neutral Bis(α -Iminopyridine)Metal Complexes of the First-Row Transition Ions (Cr, Mn, Fe, Co, Ni, Zn) and Their Monocationic Analogues: Mixed Valency Involving a Redox Noninnocent Ligand System. *J. Am. Chem. Soc.* **2008**, *130* (10), 3181–3197. <https://doi.org/10.1021/ja710663n>.
129. Hagen, V.; Dekowski, B.; Kotzur, N.; Lechler, R.; Wiesner, B.; Briand, B.; Beyermann, M. {7-[Bis(Carboxymethyl)Amino]Coumarin-4-Yl}methoxycarbonyl Derivatives for Photorelease of Carboxylic Acids, Alcohols/Phenols, Thioalcohols/Thiophenols, and Amines. *Chem. Eur. J.* **2008**, *14* (5), 1621–1627. <https://doi.org/10.1002/chem.200701142>.
130. Abou Nakad, E.; Bolze, F.; Specht, A. O-Nitrobenzyl Photoremovable Groups with Fluorescence Uncaging Reporting Properties. *Org. Biomol. Chem.* **2018**, *16* (33), 6115–6122. <https://doi.org/10.1039/c8ob01330f>.
131. Ciesienki, K. L. *Design of Photocage Ligands for Light-Activated Changes in Coordination of d-Block Transition Metals*; 2010.
132. Bonnet, S. Why Develop Photoactivated Chemotherapy? *Dalton. Trans.* **2018**, *47* (31), 10330–10343. <https://doi.org/10.1039/c8dt01585f>.
133. Givens, R. S.; Conrad, P. G.; Yousef, A. L.; Lee, J. I. Photoremovable Protecting Groups. In *CRC Handbook of: Organic Photochemistry and Photobiology, Second Edition*; 2003; pp 69–169–46. https://doi.org/10.1007/978-1-4613-2681-6_7.
134. Lu, C. A Novel Photo-Labile Caged Peptide for the Repairment of Spinal Cord Injuries; 2014.
135. Adams, S. R.; Tsien, R. Y. Controlling Cell Chemistry with Caged Compounds. *Annu. Rev. Physiol.* **1993**, *55*, 755–784. <https://doi.org/10.1146/annurev.ph.55.030193.003543>.
136. Klán, P.; Šolomek, T.; Bochet, C. G.; Blanc, A.; Givens, R.; Rubina, M.; Popik, V.; Kostikov, A.; Wirz, J. Photoremovable Protecting Groups in Chemistry and Biology: Reaction Mechanisms and Efficacy. *Chem. Rev.* **2013**, *113* (1), 119–191. <https://doi.org/10.1021/cr300177k>.
137. McCray, J. A.; Trentham, D. R. Properties and Uses of Photoreactive Caged Compounds. *Annu. Rev. Biophys. Chem.* **1989**, *18*, 239–270. <https://doi.org/10.1146/annurev.bb.18.060189.00132>.
138. Ciesienki, K. L.; Haas, K. L.; Dickens, M. G.; Tesema, Y. T.; Franz, K. J. A Photolabile Ligand for Light-Activated Release of Caged Copper. *J. Am. Chem. Soc.* **2008**, *130* (37), 12246–12247. <https://doi.org/10.1021/ja8047442>.
139. Ghosts, B. C.; Kaplan, J. H.; Forbush, B. Rapid Photolytic Release of Adenosine S³-Triphosphate from a Protected Analogue: Utilization by the Na⁺ K Pump of Human Red. *Am. Chem. Soc.* **1978**, *17* (10), 1929–1935. <https://doi.org/10.1021/bi00603a020>.
140. Carafoli, E. Intracellular Calcium Homeostasis. *Annual review of biochemistry.* 1987, pp 395–433. <https://doi.org/10.1146/annurev.bi.56.070187.002143>.
141. Tsien, R. Y. Biologically Useful Chelators That Release Ca²⁺ upon Illumination. *J. Am. Chem. Soc.* **1988**, *110* (3), 3212–3220. <https://doi.org/10.1021/ja00218a034>.
142. Ellis-davies, G. C. R. Neurobiology with Caged Calcium. *Chem. Rev.* **2008**, *108*, 1603–1613. <https://doi.org/10.1021/cr078210i>.
143. Gwizdala, C. *Design, Synthesis, and Application of Photoactive Complexes of Biologically Relevant Metals*; 2013.
144. Ciesienki, K. L.; Haas, K. L.; Franz, K. J. Development of Next-Generation Photolabile Copper Cages with Improved Copper Binding Properties. *Dalton. Trans.* **2010**, *39*, 9538–9546. <https://doi.org/10.1039/c0dt00770f>.
145. Kumbhar, A. A.; Franks, A. T.; Butcher, R. J.; Franz, K. J. Light Uncages a Copper Complex to Induce

- Nonapoptotic Cell Death. *Chem. Commun.* **2013**, 49 (24), 2460–2462. <https://doi.org/10.1039/c3cc38927h>.
146. Ciesienki, K. L.; Hyman, L. M.; Derisavifard, S.; Franz, K. J. Toward the Detection of Cellular Copper(II) by a Light-Activated Fluorescence Increase. *Inorg. Chem.* **2010**, 49 (15), 6808–6810. <https://doi.org/10.1021/ic1004165>.
147. Mbatia, H. W.; Dhammika Bandara, H. M.; Burdette, S. C. CuproCleave-1, a First Generation Photocage for Cu⁺. *Chem. Commun.* **2012**, 48 (43), 5331–5333. <https://doi.org/10.1039/c2cc31281f>.
148. Osredkar, J. Copper and Zinc, Biological Role and Significance of Copper/Zinc Imbalance. *J. Clin. Toxicol.* **2011**, s3 (1), 2–18. <https://doi.org/10.4172/2161-0495.s3-001>.
149. Kennedy, D. P.; Gwizdala, C.; Burdette, S. C. Methods for Preparing Metal Ion Photocages: Application to the Synthesis of Crowncast. *Org. Lett.* **2009**, 11 (12), 2587–2590. <https://doi.org/10.1021/ol900902z>.
150. Bandara, H. M. D.; Kennedy, D. P.; Akin, E.; Incarvito, C. D.; Burdette, S. C. Photoinduced Release of Zn²⁺ with ZinCleave-1: A Nitrobenzyl-Based Caged Complex. *Inorg. Chem.* **2009**, 48 (17), 8445–8455. <https://doi.org/10.1021/ic901062n>.
151. Bandara, H. M. D.; Walsh, T. P.; Burdette, S. C. A Second-Generation Photocage for Zn²⁺ Inspired by TPEN: Characterization and Insight into the Uncaging Quantum Yields of ZinCleave Chelators. *Chem. Eur. J.* **2011**, 17 (14), 3932–3941. <https://doi.org/10.1002/chem.201001982>.
152. Gwizdala, C.; Basa, P. N.; MacDonald, J. C.; Burdette, S. C. Increasing the Dynamic Range of Metal Ion Affinity Changes in Zn²⁺ Photocages Using Multiple Nitrobenzyl Groups. *Inorg. Chem.* **2013**, 52 (15), 8483–8494. <https://doi.org/10.1021/ic400465g>.
153. Basa, P. N.; Antala, S.; Dempski, R. E.; Burdette, S. C. A Zinc(II) Photocage Based on a Decarboxylation Metal Ion Release Mechanism for Investigating Homeostasis and Biological Signaling. *Angew. Chem. Int. Ed.* **2015**, 54 (44), 13027–13031. <https://doi.org/10.1002/anie.201505778>.
154. Basa, P. N.; Barr, C. A.; Oakley, K. M.; Liang, X.; Burdette, S. C. Zinc Photocages with Improved Photophysical Properties and Cell Permeability Imparted by Ternary Complex Formation. *J. Am. Chem. Soc.* **2019**, 141 (30), 12100–12108. <https://doi.org/10.1021/jacs.9b05504>.
155. Celina Gwizdala, Charlene V. Singh, Tracey R. Friss, J. C. M. and S. C. B. Quantifying Factors That Influence Metal Ion Release in Photocaged Complexes Using ZinCast Derivatives. *Dalton. Trans.* **2012**, 41 (26), 8162–8174. <https://doi.org/10.1039/c2dt30639e>.
156. Gwizdala, C.; Singh, C. V.; Friss, T. R.; MacDonald, J. C.; Burdette, S. C. Quantifying Factors That Influence Metal Ion Release in Photocaged Complexes Using ZinCast Derivatives. *Dalton. Trans.* **2012**, 41 (26), 8162–8174. <https://doi.org/10.1039/c2dt30135k>.
157. Gwizdala, C.; Kennedy, D. P.; Burdette, S. C. ZinCast-1: A Photochemically Active Chelator for Zn²⁺. *Chem. Commun.* **2009**, 0 (45), 6967–6969. <https://doi.org/10.1039/b913605c>.
158. Groves, J. T. The Bioinorganic Chemistry of Iron in Oxygenases and Supramolecular Assemblies. *Proc. Natl. Acad. Sci. U. S. A.* **2003**, 100 (7), 3569–3574. <https://doi.org/10.1073/pnas.0830019100>.
159. Martinez, J. S.; Zhang, G. P.; Holt, P. D.; Jung, H. T.; Carrano, C. J.; Haygood, M. G.; Butler, A. Self-Assembling Amphiphilic Siderophores from Marine Bacteria. *Science* **2000**, 287 (5456), 1245–1247. <https://doi.org/10.1126/science.287.5456.1245>.
160. Barbeau, K.; Rue, E. L.; Bruland, K. W.; Butler, A. Photochemical Cycling of Iron in the Surface Ocean Mediated by Microbial Iron(III)-Binding Ligands. *Nature* **2001**, 413 (6854), 409–413. <https://doi.org/10.1038/35096545>.
161. Kennedy, D. P.; Incarvito, C. D.; Burdette, S. C. FerriCast: A Macrocyclic Photocage for Fe³⁺. *Inorg. Chem.* **2010**, 49 (3), 916–923. <https://doi.org/10.1021/ic901182c>.
162. Mbatia, H. W.; Kennedy, D. P.; Burdette, S. C. Understanding the Relationship between Photolysis Efficiency and Metal Binding Using Argencast Photocages. *Photochem. Photobiol.* **2012**, 88 (4), 844–850. <https://doi.org/10.1111/j.1751-1097.2012.01136.x>.
163. Oun, R.; Moussa, Y. E.; Wheate, N. J. The Side Effects of Platinum-Based Chemotherapy Drugs: A Review for Chemists. *Dalton. Trans.* **2018**, 47 (19), 6645–6653. <https://doi.org/10.1039/c8dt00838h>.
164. (164) Ito, T.; Tanabe, K.; Yamada, H.; Hatta, H.; Nishimoto, S. I. Radiation- and Photo-Induced Activation of 5-Fluorouracil Prodrugs as a Strategy for the Selective Treatment of Solid Tumors. *Molecules* **2008**, 13 (10), 2370–2384. <https://doi.org/10.3390/molecules13102370>.
165. Ciesienki, K. L.; Hyman, L. M.; Yang, D. T.; Haas, K. L.; Dickens, M. G.; Holbrook, R. J.; Franz, K. J. A Photo-Caged Platinum(II) Complex That Increases Cytotoxicity upon Light Activation. *Eur. J. Inorg. Chem.* **2010**, 2010 (15), 2224–2228. <https://doi.org/10.1002/ejic.201000098>.
166. Johansson, E.; Parkinson, G. N.; Denny, W. A.; Neidle, S. Studies on the Nitroreductase Prodrug-Activating System. Crystal Structures of Complexes with the Inhibitor Dicoumarol and Dinitrobenzamide Prodrugs and of the Enzyme Active Form. *J. Med. Chem.* **2003**, 46 (19), 4009–4020. <https://doi.org/10.1021/jm030843b>.
167. A. M. Rauth, T. M. and V. M. Bioreductive Therapies: An Overview of Drugs and Their Mechanisms of Action. *Int. J. Radiat. Oncol. Biol. Phys.* **2015**, 42 (4), 755–762. <https://doi.org/10.4324/9781315703237-41>.
168. Padda, R. S.; Wang, C.; Hughes, J. B.; Kutty, R.; Bennett, G. N. Mutagenicity of Nitroaromatic Degradation Compounds. *Environ. Toxicol. Chem.* **2003**, 22 (10), 2293–2297. <https://doi.org/10.1897/02-220>.
169. Li, Z.; Li, X.; Gao, X.; Zhang, Y.; Shi, W.; Ma, H. Nitroreductase Detection and Hypoxic Tumor Cell Imaging by a Designed Sensitive and Selective Fluorescent Probe, 7-[(5-Nitrofuranyl)Methoxy]-3 H -Phenoxazin-3-One. *Anal. Chem.* **2013**, 85 (8), 3926–3932. <https://doi.org/10.1021/ac400750r>.
170. Cui, L.; Zhong, Y.; Zhu, W.; Xu, Y.; Du, Q.; Wang, X.; Qian, X.; Xiao, Y. A New Prodrug-Derived Ratiometric Fluorescent Probe for Hypoxia: High Selectivity of Nitroreductase and Imaging in Tumor Cell. *Org. Lett.* **2011**, 13 (5), 928–931. <https://doi.org/10.1021/ol102975t>.
171. O kuda, K.; Okabe, Y.; Kadonosono, T.; Ueno, T.;

- Youssif, B. G. M.; Kizaka-Kondoh, S.; Nagasawa, H. 2-Nitroimidazole-Tricarbo-cyanine Conjugate As a Near-Infrared Fluorescent Probe for in Vivo Imaging of Tumor Hypoxia. *Bioconjugate Chem.* **2012**, *23* (3), 324–329. <https://doi.org/10.1021/bc2004704>.
172. Gebremedhin, K. H.; Li, Y.; Yao, Q.; Xiao, M.; Gao, F.; Fan, J.; Du, J.; Long, S.; Peng, X. Development of a Red-Light Emission Hypoxia-Sensitive Two-Photon Fluorescent Probe for: In Vivo Nitroreductase Imaging. *J. Mater. Chem. B* **2019**, *7* (3), 408–414. <https://doi.org/10.1039/c8tb02635a>.
173. Li, Z.; He, X.; Wang, Z.; Yang, R.; Shi, W.; Ma, H. In Vivo Imaging and Detection of Nitroreductase in Zebrafish by a New Near-Infrared Fluorescence off-on Probe. *Biosens. Bioelectron.* **2015**, *63*, 112–116. <https://doi.org/10.1016/j.bios.2014.07.024>.
174. Sha, X. L.; Yang, X. Z.; Wei, X. R.; Sun, R.; Xu, Y. J.; Ge, J. F. A Mitochondrial/Lysosome-Targeting Fluorescence Probe Based on Azonia-Cyanine Dye and Its Application in Nitroreductase Detection. *Sensors Actuators, B Chem.* **2020**, *307* (October 2019), 127653–127661. <https://doi.org/10.1016/j.snb.2019.127653>.
175. Elmes, R. B. P. Bioreductive Fluorescent Imaging Agents: Applications to Tumour Hypoxia. *Chem. Commun.* **2016**, *52* (58), 8935–8956. <https://doi.org/10.1039/c6cc01037g>.
176. Chevalier, A.; Zhang, Y.; Khdour, O. M.; Kaye, J. B.; Hecht, S. M. Mitochondrial Nitroreductase Activity Enables Selective Imaging and Therapeutic Targeting. *J. Am. Chem. Soc.* **2016**, *138* (37), 12009–12012. <https://doi.org/10.1021/jacs.6b06229>.
177. Oxygen-insensitive NAD(P)H nitroreductase NfsB <https://www.ebi.ac.uk/interpro/entry/InterPro/IPR033878/#PUB00081527>.
178. Bryant, D. W.; McCalla, D. R.; Leeksa, M.; Laneville, P. Type I Nitroreductases of *Escherichia Coli*. *Can. J. Microbiol.* **1981**, *27* (1), 81–86. <https://doi.org/10.1139/m81-013>.
179. Jeong, J. Y.; Mukhopadhyay, A. K.; Akada, J. K.; Dailidienne, D.; Hoffman, P. S.; Berg, D. E. Roles of FrxA and RdxA Nitroreductases of *Helicobacter Pylori* in Susceptibility and Resistance to Metronidazole. *J. Bacteriol.* **2001**, *183* (17), 5155–5162. <https://doi.org/10.1128/JB.183.17.5155-5162.2001>.
180. Zenno, S.; Saigo, K.; Kanoh, H.; Inouye, S. Identification of the Gene Encoding the Major NAD(P)H-Flavin Oxidoreductase of the Bioluminescent Bacterium *Vibrio Fischeri* ATCC 7744. *J. Bacteriol.* **1994**, *176* (12), 3536–3543. <https://doi.org/10.1128/jb.176.12.3536-3543.1994>.
181. Brennecke, B.; Wang, Q.; Zhang, Q.; Hu, H. Y.; Nazaré, M. An Activatable Lanthanide Luminescent Probe for Time-Gated Detection of Nitroreductase in Live Bacteria. *Angew. Chem. Int. Ed.* **2020**, *59* (22), 8512–8516. <https://doi.org/10.1002/anie.202002391>.
182. James, A. L.; Perry, J. D.; Jay, C.; Monget, D.; Rasburn, J. W.; Gould, F. K. Fluorogenic Substrates for the Detection of Microbial Nitroreductases. *Let. Appl. Microbiol.* **2001**, *33* (6), 403–408. <https://doi.org/10.1046/j.1472-765X.2001.01021.x>.
183. Wangngae, S.; Pewklang, T.; Chansaenpak, K.; Ganta, P.; Worakaensai, S.; Siwawannapong, K.; Kluaiphannang, S.; Nantapong, N.; Lai, R. Y.; Kamkaew, A. A Chalcone-Based Fluorescent Responsive Probe for Selective Detection of Nitroreductase Activity in Bacteria. *New J. Chem.* **2021**, *45* (26), 11566–11573. <https://doi.org/10.1039/d1nj01794b>.
184. Williams, E. M.; Little, R. F.; Mowday, A. M.; Rich, M. H.; Chan-Hyams, J. V. E.; Copp, J. N.; Smail, J. B.; Patterson, A. V.; Ackerley, D. F. Nitroreductase Gene-Directed Enzyme Prodrug Therapy: Insights and Advances toward Clinical Utility. *Biochem. J.* **2015**, *471* (2), 131–153. <https://doi.org/10.1042/BJ20150650>.
185. Olive, P. L.; Durand, R. E. Fluorescent Nitroheterocycles for Identifying Hypoxic Cells. *Cancer Res.* **1983**, *43* (7), 3276–3280.
186. Manuscript, A. Bioreductive Fluorescent Imaging Agents: Applications to Tumour Hypoxia. *Chem. Commun.* **2016**, *52*, 8935–8956. <https://doi.org/10.1039/C6CC01037G>.
187. Stratford, M. R. L.; Clarke, E. D.; Hodgkiss, R. J.; Middleton, R. W.; Wardman, P. Nitroaryl Compounds as Potential Fluorescent Probes for Hypoxia. II. Identification and Properties of Reductive Metabolites. *Int. J. Radiat. Oncol. Biol. Phys.* **1984**, *10* (8), 1353–1356. [https://doi.org/10.1016/0360-3016\(84\)90347-X](https://doi.org/10.1016/0360-3016(84)90347-X).
188. Wardman, P.; Clarke, E. D.; Hodgkiss, R. J.; Middleton, R. W.; Parrick, J.; Stratford, M. R. L. Nitroaryl Compounds as Potential Fluorescent Probes for Hypoxia. I. Chemical Criteria and Constraints. *Int. J. Radiat. Oncol. Biol. Phys.* **1984**, *10* (8), 1347–1351. [https://doi.org/10.1016/0360-3016\(84\)90346-8](https://doi.org/10.1016/0360-3016(84)90346-8).
189. Begg, A. C.; Engelhardt, E. L.; Hodgkiss, R. J.; McNally, N. J.; Terry, N. H. A.; Wardman, P. Nitroakridin 3582: A Fluorescent Nitroacridine Stain for Identifying Hypoxic Cells. *Br. J. Radiol.* **1983**, *56* (672), 970–973. <https://doi.org/10.1259/0007-1285-56-672-970>.
190. Hodgkiss, R. J.; Begg, A. C.; Middleton, R. W.; Parrick, J.; Stratford, M. R. L.; Wardman, P.; Wilson, G. D. Fluorescent Markers for Hypoxic Cells. A Study of Novel Heterocyclic Compounds That Undergo Bio-Reductive Binding. *Biochem. Pharmacol.* **1991**, *41* (4), 533–541. [https://doi.org/10.1016/0006-2952\(91\)90625-F](https://doi.org/10.1016/0006-2952(91)90625-F).
191. Liu, Y.; Xu, Y.; Qian, X.; Liu, J.; Shen, L.; Li, J.; Zhang, Y. Novel Fluorescent Markers for Hypoxic Cells of Naphthalimides with Two Heterocyclic Side Chains for Bioreductive Binding. *Bioorg. Med. Chem.* **2006**, *14* (9), 2935–2941. <https://doi.org/10.1016/j.bmc.2005.12.012>.
192. Liu, Y.; Xu, Y.; Qian, X.; Xiao, Y.; Liu, J.; Shen, L.; Li, J.; Zhang, Y. Synthesis and Evaluation of Novel 8-Oxo-8H-Cyclopenta[a]Acenaphthylene-7-Carbonitriles as Long-Wavelength Fluorescent Markers for Hypoxic Cells in Solid Tumor. *Bioorg. Med. Chem. Lett.* **2006**, *16* (6), 1562–1566. <https://doi.org/10.1016/j.bmlc.2005.12.031>.
193. Cui, L.; Zhong, Y.; Zhu, W.; Xu, Y.; Du, Q.; Wang, X.; Qian, X.; Xiao, Y. A New Prodrug-Derived Ratiometric Fluorescent Probe for Hypoxia: High Selectivity of Nitroreductase and Imaging in Tumor Cell. *Org. Lett.* **2011**, *13* (5), 928–931. <https://doi.org/10.1021/ol102975t>.
194. Yoon, S. A.; Chun, J.; Kang, C.; Lee, M. H. Self-Calibrating Bipartite Fluorescent Sensor for Nitroreductase Activity and Its Application to Cancer and Hypoxic Cells. *ACS Appl. Bio Mater.* **2021**, *4* (3), 2052–2057. <https://doi.org/10.1021/acsbm.0c01085>.

195. Xu, A.; Tang, Y.; Lin, W. Endoplasmic Reticulum-Targeted Two-Photon Turn-on Fluorescent Probe for Nitroreductase in Tumor Cells and Tissues. *Spectrochim. Acta - Part A Mol. Biomol. Spectrosc.* **2018**, *204*, 770–776. <https://doi.org/10.1016/j.saa.2018.05.092>.
196. Zhang, Z.; Lv, T.; Tao, B.; Wen, Z.; Xu, Y.; Li, H.; Liu, F.; Sun, S. A Novel Fluorescent Probe Based on Naphthalimide for Imaging Nitroreductase (NTR) in Bacteria and Cells. *Bioorg. Med. Chem.* **2020**, *28* (3), 115280. <https://doi.org/10.1016/j.bmc.2019.115280>.
197. Zou, Y.; Chen, X.; Cheng, Z.; Chen, H.; Wu, J.; Liu, H.; Ye, Q. Evaluation of Nitroreductase Activity in Nasopharyngeal Carcinoma Progression by an Activatable Two-Photon Fluorescent Probe. *Spectrochim. Acta - Part A Mol. Biomol. Spectrosc.* **2022**, *281* (July), 121616. <https://doi.org/10.1016/j.saa.2022.121616>.
198. Guo, T.; Cui, L.; Shen, J.; Zhu, W.; Xu, Y.; Qian, X. A Highly Sensitive Long-Wavelength Fluorescence Probe for Nitroreductase and Hypoxia: Selective Detection and Quantification. *Chem. Commun.* **2013**, *49* (92), 10820–10822. <https://doi.org/10.1039/c3cc45367g>.
199. Nakata, E.; Yukimachi, Y.; Kariyazono, H.; Im, S.; Abe, C.; Uto, Y.; Maezawa, H.; Hashimoto, T.; Okamoto, Y.; Hori, H. Design of a Bioreductively-Activated Fluorescent PH Probe for Tumor Hypoxia Imaging. *Bioorg. Med. Chem.* **2009**, *17* (19), 6952–6958. <https://doi.org/10.1016/j.bmc.2009.08.037>.
200. Okuda, K.; Okabe, Y.; Kadonosono, T.; Ueno, T.; Youssif, B. G. M.; Kizaka-Kondoh, S.; Nagasawa, H. 2-Nitroimidazole-Tricarbocyanine Conjugate as a near-Infrared Fluorescent Probe for in Vivo Imaging of Tumor Hypoxia. *Bioconjugate Chem.* **2012**, *23* (3), 324–329. <https://doi.org/10.1021/bc2004704>.
201. Shi, Y.; Zhang, S.; Zhang, X. A Novel Near-Infrared Fluorescent Probe for Selectively Sensing Nitroreductase (NTR) in an Aqueous Medium. *Analyst* **2013**, *138* (7), 1952–1955. <https://doi.org/10.1039/c3an36807f>.
202. Yuan, J.; Xu, Y. Q.; Zhou, N. N.; Wang, R.; Qian, X. H.; Xu, Y. F. A Highly Selective Turn-on Fluorescent Probe Based on Semi-Cyanine for the Detection of Nitroreductase and Hypoxic Tumor Cell Imaging. *RSC Adv.* **2014**, *4* (99), 56207–56210. <https://doi.org/10.1039/c4ra10044a>.
203. Xue, C.; Lei, Y.; Zhang, S.; Sha, Y. A Cyanine-Derived “Turn-on” Fluorescent Probe for Imaging Nitroreductase in Hypoxic Tumor Cells. *Anal. Methods* **2015**, *7* (24), 10125–10128. <https://doi.org/10.1039/c5ay02312b>.
204. Ji, Y.; Wang, Y.; Zhang, N.; Xu, S.; Wang, Q.; Zhang, Q.; Hu, H. Cell-Permeable Fluorogenic Probes for Identification and Imaging Nitroreductases in Live Bacterial Cells Cell-Permeable Fluorogenic Probes for Identification and Imaging Nitroreductases in Live Bacterial Cells. *J. Org. Chem.* **2018**, *84* (3), 1299–1309. <https://doi.org/10.1021/acs.joc.8b02746>.
205. Wang, Y.; Zhang, L.; Huang, Y.; Wang, X.; Zhang, L.; Chen, L. Rational Design of a Nitroreductase-Activatable Two-Photon Fluorescent Probe for Hypoxia Imaging in Cell and in Vivo. *Sensors Actuators B Chem.* **2020**, *310*, 127755. <https://doi.org/10.1016/j.snb.2020.127755>.
206. Liu, T.; Wang, Y.; Feng, L.; Tian, X.; Cui, J.; Yu, Z.; Wang, C.; Zhang, B.; James, T. D.; Ma, X. 2D Strategy for the Construction of an Enzyme-Activated NIR Fluorophore Suitable for the Visual Sensing and Profiling of Homologous Nitroreductases from Various Bacterial Species. *ACS Sensors* **2021**, *6*, 3348–3356. <https://doi.org/10.1021/acssensors.1c01216>.
207. Wu, L. L.; Wang, Q.; Wang, Y.; Zhang, N.; Zhang, Q.; Hu, H. Y. Rapid Differentiation between Bacterial Infections and Cancer Using a Near-Infrared Fluorogenic Probe. *Chem. Sci.* **2020**, *11* (12), 3141–3145. <https://doi.org/10.1039/d0sc00508h>.
208. Zhang, X.; Gao, Z.; Xia, Y.; Dong, Q.; Cao, Y.; Jia, Q.; Sun, F.; Li, Z.; Tang, C.; Yu, J. Insight into the Spatial Interaction of D- π -A Bridge Derived Cyanines and Nitroreductase for Fluorescent Cancer Hypoxia Detection. *Spectrochim. Acta - Part A Mol. Biomol. Spectrosc.* **2022**, *273*, 121031. <https://doi.org/10.1016/j.saa.2022.121031>.
209. Lin, Q.; Li, C.; Wang, L.; Cai, H.; Tang, L.; Gu, Y. Ultrasensitive Near-Infrared Fluorescence Probe Activated by Nitroreductase for in Vivo Hypoxia Detection. *Sensors Actuators B Chem.* **2022**, *371* (July), 132521. <https://doi.org/10.1016/j.snb.2022.132521>.
210. Evans, S. M.; Kim, K.; Moore, C. E.; Imam Uddin, M.; Capozzi, M. E.; Craft, J. R.; Sulikowski, G. A.; Jayagopal, A. Molecular Probes for Imaging of Hypoxia in the Retina. *Bioconjugate Chem.* **2014**, *25*, 2030–2037. <https://doi.org/10.1021/bc500400z>.
211. Ying Zhou, Kondapa Naidu Bobba, Xue Wei Lv, Dan Yang, Niithya Velusamy, J. F. Z. S. B. Biotinylated Piperazine-Rhodol Derivative: A ‘Turn-On’ Probe for Nitroreductase Triggered Hypoxia Imaging. *Analyst* **2017**, *142* (2), 345–350. <https://doi.org/10.1039/C6AN02107G>.
212. Shenzheng Luo, Rongfeng Zou, Junchen Wu, and M. P. L. A Probe for the Detection of Hypoxic Cancer Cells. *ACS Sensors* **2017**, *2* (8), 1139–1145. <https://doi.org/10.1021/acssensors.7b00171>.
213. More, K. N.; Lim, T.; Kim, S.; Kang, J.; Inn, K.; Chang, D. Characteristics of New Bioreductive Fluorescent Probes Based on the Xanthene Fluorophore: Detection of Nitroreductase and Imaging of Hypoxic Cells. *Dye. Pigment.* **2018**, *151*, 245–253. <https://doi.org/10.1016/j.dyepig.2018.01.008>.
214. Wang, Y.; Meng, X.; Ma, A.; Sun, M.; Jiao, S.; Wang, C. Molecular and Biomolecular Spectroscopy Rhodol-Derived Turn-on Fluorescent Chemosensor for Ultrasensitive Detection of Nitroreductase Activity in Bacteria and Bioimaging in Oral Cancer Cells. *Spectrochim. Acta Part A Mol. Biomol. Spectrosc.* **2022**, *270*, 120836. <https://doi.org/10.1016/j.saa.2021.120836>.
215. Mi, Z.; Liu, L.; Zhao, Y.; Guan, J. Selective Colorimetric and Fluorescence Detection of Nitroreductase Enzymes in Living Cells. *Int. J. Biol. Macromol.* **2020**, *164*, 932–938. <https://doi.org/10.1016/j.ijbiomac.2020.07.148>.
216. Fang, Y.; Shi, W.; Hu, Y.; Li, X.; Ma, H. A Dual-Function Fluorescent Probe for Monitoring the Degrees of Hypoxia in Living Cells: Via the Imaging of Nitroreductase and Adenosine Triphosphate. *Chem. Commun.* **2018**, *54* (43), 5454–5457. <https://doi.org/10.1039/c8cc02209g>.
217. Gruber, T. D.; Krishnamurthy, C.; Grimm, J. B.; Tadross, M. R.; Wysocki, L. M.; Gartner, Z. J.; Lavis, L. D. Cell-Specific Chemical Delivery Using a Selective Nitroreductase-Nitroaryl Pair. *ACS Chem.*

- Biol.* **2018**, *13* (10), 2888–2896. <https://doi.org/10.1021/acscchembio.8b00524>.
218. Chumakov, S. P.; Mironiuk, V. B.; Yuriy, N.; Muzafarov, A. M.; Martynov, V. I. BODIPY-Based Dye for No-Wash Live-Cell Staining and Imaging. *Biotechniques* **2017**, *63*, 77–80. <https://doi.org/10.2144/000114577>.
219. Loudet, A.; Burgess, K. BODIPY Dyes and Their Derivatives: Syntheses and Spectroscopic Properties. *Chem. Rev.* **2007**, *107* (11), 4891–4932. <https://doi.org/10.1021/cr078381n>.
220. Ulrich, G.; Ziessel, R.; Harriman, A. The Chemistry of Fluorescent Bodipy Dyes: Versatility Unsurpassed. *Angew. Chem. Int. Ed.* **2008**, *47* (7), 1184–1201. <https://doi.org/10.1002/anie.200702070>.
221. Lee, J. S.; Kang, N. Y.; Yun, K. K.; Samanta, A.; Feng, S.; Hyeong, K. K.; Vendrell, M.; Jung, H. P.; Chang, Y. T. Synthesis of a BODIPY Library and Its Application to the Development of Live Cell Glucagon Imaging Probe. *J. Am. Chem. Soc.* **2009**, *131* (29), 10077–10082. <https://doi.org/10.1021/ja9011657>.
222. Niu, L. Y.; Guan, Y. S.; Chen, Y. Z.; Wu, L. Z.; Tung, C. H.; Yang, Q. Z. BODIPY-Based Ratiometric Fluorescent Sensor for Highly Selective Detection of Glutathione over Cysteine and Homocysteine. *J. Am. Chem. Soc.* **2012**, *134* (46), 18928–18931. <https://doi.org/10.1021/ja309079f>.
223. Xu, J.; Sun, S.; Li, Q.; Yue, Y.; Li, Y.; Shao, S. A Rapid Response “Turn-On” Fluorescent Probe for Nitroreductase Detection and Its Application in Hypoxic Tumor Cell Imaging. *Analyst* **2015**, *140* (2), 574–581. <https://doi.org/10.1039/c4an01934b>.
224. Ulrich, G.; Ziessel, R. Convenient and Efficient Synthesis of Functionalized Oligopyridine Ligands Bearing Accessory Pyromethene-BF₂ Fluorophores. *J. Org. Chem.* **2004**, *69* (6), 2070–2083. <https://doi.org/10.1021/jo035825g>.
225. Alamiry, M. A. H.; Harriman, A.; Mallon, L. J.; Ulrich, G.; Ziessel, R. Energy- and Charge-Transfer Processes in a Perylene–BODIPY–Pyridine Tripartite Array. *European J. Org. Chem.* **2008**, *2008* (16), 2774–2782. <https://doi.org/10.1002/ejoc.200800159>.
226. Harriman, A.; Mallon, L. J.; Ulrich, G.; Ziessel, R. Rapid Intersystem Crossing in Closely-Spaced but Orthogonal Molecular Dyads. *ChemPhysChem* **2007**, *8* (8), 1207–1214. <https://doi.org/10.1002/cphc.200700060>.
227. Wang, D.; Miyamoto, R.; Shiraishi, Y.; Hirai, T. BODIPY-Conjugated Thermoresponsive Copolymer as a Fluorescent Thermometer Based on Polymer Microviscosity. *Langmuir* **2009**, *25* (22), 13176–13182. <https://doi.org/10.1021/la901860x>.
228. Xu, J.; Li, Q.; Yue, Y.; Guo, Y.; Shao, S. A Water-Soluble BODIPY Derivative as a Highly Selective “Turn-On” Fluorescent Sensor for H₂O₂ Sensing in Vivo. *Biosens. Bioelectron.* **2014**, *56*, 58–63. <https://doi.org/10.1016/j.bios.2013.12.065>.
229. Zhang, S.; Wu, T.; Fan, J.; Li, Z.; Jiang, N.; Wang, J.; Dou, B.; Sun, S.; Song, F.; Peng, X. A BODIPY-Based Fluorescent Dye for Mitochondria in Living Cells, with Low Cytotoxicity and High Photostability. *Org. Biomol. Chem.* **2013**, *11* (4), 555–558. <https://doi.org/10.1039/c2ob26911b>.
230. Jiang, N.; Fan, J.; Liu, T.; Cao, J.; Qiao, B.; Wang, J.; Gao, P.; Peng, X. A Near-Infrared Dye Based on BODIPY for Tracking Morphology Changes in Mitochondria. *Chem. Commun.* **2013**, *49* (90), 10620–10622. <https://doi.org/10.1039/c3cc46143b>.
231. Wang, S.; Liu, H.; Mack, J.; Tian, J.; Zou, B.; Lu, H.; Li, Z.; Jiang, J.; Shen, Z. A BODIPY-Based “turn-on” Fluorescent Probe for Hypoxic Cell Imaging. *Chem. Commun.* **2015**, *51* (69), 13389–13392. <https://doi.org/10.1039/c5cc05139h>.
232. Gorbатов, S. A., Uvarov, D.Y., Scherbakov, A.M., Zavarzin, I.V., Volkova, Y.A., Romieua, A. Novel Water-Soluble Far-Rednitroreductase-Responsive Bodipy-Based Fluorescent Probe for the Detection of Hypoxic Status in A549 Non-Small Cell Lung Cancer Cells. *ChemRxiv* **2020**, 1–9.
233. Kim, T. Il; Kim, H.; Choi, Y.; Kim, Y. Meso-Ester BODIPYs for the Imaging of Hypoxia in Tumor Cells. *Sensors Actuators, B Chem.* **2017**, *249*, 229–234. <https://doi.org/10.1016/j.snb.2017.04.093>.
234. Zhu, N.; Xu, G.; Wang, R.; Zhu, T.; Tan, J.; Gu, X.; Zhao, C. Precise Imaging of Mitochondria in Cancer Cells by Real-Time Monitoring of Nitroreductase Activity with a Targetable and Activatable Fluorescent Probe. *Chem. Commun.* **2020**, *56* (56), 7761–7764. <https://doi.org/10.1039/d0cc00494d>.
235. Karan, S.; Cho, M. Y.; Lee, H.; Lee, H.; Park, H. S.; Sundararajan, M.; Sessler, J. L.; Hong, K. S. Near-Infrared Fluorescent Probe Activated by Nitroreductase for in Vitro and in Vivo Hypoxic Tumor Detection. *J. Med. Chem.* **2021**, *64* (6), 2971–2981. <https://doi.org/10.1021/acs.jmedchem.0c02162>.
236. Li, X.; Geng, P.; Hong, X.; Sun, Z.; Liu, G. Detecting Mycobacterium Tuberculosis Using a Nitrofuranyl Calanolide – Trehalose Probe Based on Nitroreductase Rv2466c. *Chem. Commun.* **2021**, *57*, 13174–13177. <https://doi.org/10.1039/d1cc05187c>.
237. Liu, Y.; Zhang, L.; Nazare, M.; Yao, Q.; Hu, H. Y. A Novel Nitroreductase-Enhanced MRI Contrast Agent and Its Potential Application in Bacterial Imaging. *Acta Pharm. Sin. B* **2018**, *8* (3), 401–408. <https://doi.org/10.1016/j.apsb.2017.11.001>.
238. Mazuryk, O.; Maciuszek, M.; Stochel, G.; Suzenet, F.; Brindell, M. 2-Nitroimidazole-Ruthenium Polypyridyl Complex as a New Conjugate for Cancer Treatment and Visualization. *J. Inorg. Biochem.* **2014**, *134*, 83–91. <https://doi.org/10.1016/j.jinorgbio.2014.02.001>.
239. Gao, F.; Chao, H.; Zhou, F.; Yuan, Y. X.; Peng, B.; Ji, L. N. DNA Interactions of a Functionalized Ruthenium(II) Mixed-Polypyridyl Complex [Ru(Bpy)₂ppd]²⁺. *J. Inorg. Biochem.* **2006**, *100* (9), 1487–1494. <https://doi.org/10.1016/j.jinorgbio.2006.04.008>.
240. Thibon, A.; Pierre, V. C. Principles of Responsive Lanthanide-Based Luminescent Probes for Cellular Imaging. *Anal. Bioanal. Chem.* **2009**, *394* (1), 107–120. <https://doi.org/10.1007/s00216-009-2683-2>.
241. Karan, S.; Cho, M. Y.; Lee, H.; Park, H. S.; Han, E. H.; Song, Y.; Lee, Y.; Kim, M.; Cho, J. H.; Sessler, J. L.; et al. Hypoxia-Responsive Luminescent CEST MRI Agent for In Vitro and In Vivo Tumor Detection and Imaging. *J. Med. Chem.* **2022**, *65* (10), 7106–7117. <https://doi.org/10.1021/acs.jmedchem.1c01745>.

7. About the author(s)



Dr. Deepti U. Kirtani received her Ph.D. in 2022 under the supervision of Dr. Anupa A. Kumbhar from Department of Chemistry, Savitribai Phule Pune University, Pune. Her dissertation 'Investigating the stimulus responsive uncaging of iron(III), copper(II) and platinum(II) complexes on antiproliferative activity' was focused on design and synthesis of fluorophore-tagged stimulus-responsive (UV light, pH and enzyme) metal complexes, explore their uncaging mechanisms and antiproliferative activity.



Dr. Anupa A. Kumbhar is an Associate Professor at the Department of Chemistry, Savitribai Phule Pune University (SPPU), Pune. Her group at SPPU is engaged in developing metal-based antibacterial agents, fluorophore-labelled metal complexes for bioimaging, and sensors for environmental and biosensing applications.

Article Note: A collection of invited papers based on *Award Lecture* presentations in the International webinar *Science Beyond Boundary: Invention, Discovery, Innovation and Society 'Rasyan 14'* held online on August 20, 2022.